

*In the name of Allah,
the Most Beneficent,
the Most Merciful*

Peristaltic Motion of Jeffrey Nanofluid in a Channel with Slip Condition

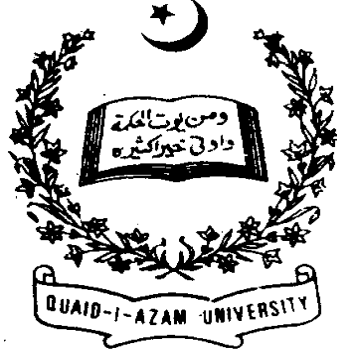


By

Maryam Shafique

Department of Mathematics
Quaid-I-Azam University
Islamabad, Pakistan
2016

Peristaltic Motion of Jeffrey Nanofluid in a Channel with Slip Condition



By

Maryam Shafique

Supervised By

Prof. Dr. Muhammad Ayub

Department of Mathematics
Quaid-I-Azam University
Islamabad, Pakistan
2016

Peristaltic Motion of Jeffrey Nanofluid in a Channel with Slip Condition



By
Maryam Shafique

A thesis submitted in the partial fulfillment of the requirement

for the degree of

MASTER OF PHILOSOPHY

IN

MATHEMATICS

Supervised By

Prof. Dr. Muhammad Ayub

Department of Mathematics

Quaid-I-Azam University

Islamabad, Pakistan

2016

Peristaltic Motion of Jeffrey Nanofluid in a Channel with Slip Condition

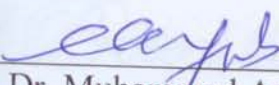
By


Maryam Shafique

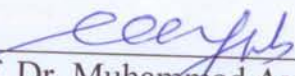
CERTIFICATE

A THESIS SUBMITTED IN THE PARTIAL FULFILLMENT OF THE
REQUIREMENTS FOR THE DEGREE OF THE MASTER OF
PHILOSOPHY

We accept this thesis as conforming to the required standard

1. 
Prof. Dr. Muhammad Ayub
(Supervisor)

2. 
Dr. Meraj Mustafa
(External)

3. 
Prof. Dr. Muhammad Ayub
(Chairman)

**Department of Mathematics
Quaid-i-Azam University
Islamabad, Pakistan
2016**

*Dedicated to my
Ammi jan and Papa
May Almighty ALLAH Bless them
and Protect them, Ameen.*

ACKNOWLEDGMENT

All praise is for Allah Almighty, the Creator, the Glorious and the Merciful Lord, who guide me in darkness, helps me in difficulties and enable me to view stumbling blocks as stepping stones to the stars to reach the ultimate stage with courage. I am nothing without my Allah but I can achieve everything with His assistance. All of my veneration goes to our beloved Prophet Hazrat Muhammad ﷺ the source of humanity, kindness and guidance for the whole creatures and who declared it an obligatory duty of every Muslim to seek and acquire knowledge. May Allah shower His countless blessings upon Muhammad ﷺ, His family and companions.

I would like to convey my profound and cordial gratitude to my honourable supervisor Prof. Dr. Muhammad Ayub and Chairman Prof. Dr. Tasawar Hayat whose generous suggestions, kind control, guidance, cooperation, encouragement and advices were greatly useful in completing this crucial task. I am also thankful to my respectable teachers Dr. Sohail Nadeem, Dr. Masood khan, Dr. Khalid Saifullah, Dr. Malik Muhammad Yousaf for their kindness and support.

My family deserves special thanks and appreciation for their inseparable support and prayers. My mother in the first place is the person whose guidance, support, encouragement and never ending prayers are the root of success, confidence and inspiration throughout my life. My great father always supported me and prayed for me in any hurdles. My heartfelt appreciations are dedicated to my sisters (Sahar api, Saba Baji), my nephews (Masharib, Abdullah, Usman, AbdulHadi), my niece (Amna Doll) and my dadi (late) whose constant prayers and love is the source of success throughout my career.

I gratefully acknowledge the invaluable suggestions and generous guidance of my coordinator Ms. Anum Tanveer. May Allah bless u anum baji. I am also thankful to my seniors Ms. Hina Zahir, Ms. Sadia Ayub and Mr. Farooq. I offer my cordial thanks to my seniors Ms. Maria Imtiaz and Ms. Maimona Rafiq for being my well-wisher. I will never forget their help and suggestions during my research work. I also owe my sincere thanks to my research fellows and friends Sumaira Qayyum, Rija Iqbal, Sadaf Nawaz, Sumaira Jabeen, Qurat-ul-Ain and Gulnaz for their suggestions and profic discussions. The time spent with my seniors and friends will always cherish my memories.

I am also thankful to all those people who loved me, cared for me and directly or indirectly helped me during my research work.

MARYAM SHAFIQUE

2ND AUGUST 2016

PREFACE

Peristaltic activity has great value in many physiological processes and industries. Peristalsis can occur due to contraction and expansion of flexible boundaries. In other words this activity includes passing down, mixing and transporting materials through contraction or expansion of the waves propagating along the channel walls. It has wide applications in medical industry and chemical processes. Typical examples in this direction include in distillation towers and fixed-bed reactors, urine transport from kidney to bladder through the ureter, transport of lymph in the lymphatic vessels, swallowing food through the esophagus, the movement of chyme in the gastrointestinal tract, ovum movement in the fallopian tube, transport of corrosive fluids, sanitary fluid transport and blood pumps in heart lung machine etc. The worms utilize peristalsis for locomotion. Latham [1] and Shapiro et al. [2] initiated works on peristalsis of viscous fluids via theoretical and experimental approaches. Later on many researchers put forward their research on this topic by considering different kinds of fluid models, no-slip/ partial slip condition and one or more assumptions of long wavelength, low Reynolds number, small amplitude ratio, small wave number etc. Especially the magnetohydrodynamics (MHD) peristaltic transport of fluid in a channel are quite important with reference to conductive physiological materials for example the blood, blood pump machines and with the need of both experimental and theoretical research for operation of peristaltic MHD compressor. Concept of magnetohydrodynamics is useful in Magnetic Resonance Imaging (MRI) when a patient undergoes in a height static magnetic field. On the other hand the heat transfer in peristalsis is useful in the oxygenation processes. Such concept is further important in the industrial applications like sanitary fluid transport and transport of corrosive materials where the fluid contact with the machinery parts is prohibited. Having all such aspects in mind many authors in past analyzed the peristaltic flows in detail (see [3- 16]). Nadeem and Akbar [17] studied influence of radially varying MHD on the peristaltic flow in an annulus. Ellahi and Hussain [18] analyzed effects of MHD and partial slip on peristaltic flow of Jeffrey fluid in a rectangular duct. Ali et al. [19] presented numerical simulation for peristaltic flow of a biorheological fluid with shear dependent viscosity in a curved channel.

Mixed convection occurs in vertical channels for improvement of cooling systems in engineering. Analysis of heat transfer with MHD and mixed convection in vertical channels has great applications in solar energy collection, chemical reactions and cooling systems. Sheikholeslami et al. [20] analyzed simulation of MHD CuO-water nanofluid flow and convective heat transfer using Lorentz force. Abbasi et al. [21] discussed effects of inclined magnetic field and Joule heating in mixed convective flows of non-Newtonian fluids. Mustafa et al. [22] analyzed Soret and Dufour effects in the mixed convective peristaltic flow of fourth grade fluid. Soret and Dufour effects in mixed convective peristalsis of viscous nanofluids are examined by Hayat et al. [23]. Srinivas and Muthuraj [24] addressed mixed convective peristalsis in presence of chemical reaction. Heat and mass transfer analysis in mixed convective peristaltic transport of viscous fluid in an asymmetric channel is studied by Srinivas et al. [25]. Peristaltic transport has not been conducted well in connection with elastic behavior of the walls. Wall properties such as elastic tension and damping are of immense importance in practical situations. Hence this dissertation is designed to explore the slip and Joule heating effects on peristalsis of Jeffrey nanofluid in a channel with compliant walls. The organization of dissertation is as follows:

Chapter one describes the fundamental laws and definitions regarding the concepts used in the chapters two and three. Chapter two refers to the study of slip and wall properties simultaneously on peristaltic flow of nanofluid. This chapter concerns the review of article [13] proposed by Hayat et al. Chapter three deals with mixed convective peristaltic flow of Jeffrey nanofluid in a compliant walls channel. Analysis has been carried out with compliant walls and slip conditions. Thermal radiation effect is present. Joule heating is taken into account. Graphical results are plotted numerically to analyze the behavior of sundry parameters on temperature, velocity, nanoparticle concentration and heat transfer coefficient.

Contents

1	Definitions and equations related to flow analysis	4
1.1	Introduction	4
1.2	Basic concepts of fluid	4
1.2.1	Fluid	4
1.2.2	Fluid mechanics	4
1.2.3	Newtonian fluid	5
1.2.4	Non-Newtonian fluid	6
1.2.5	Rate type fluid models	7
1.2.6	Fluid density	7
1.2.7	Fluid viscosity	8
1.3	Pressure	8
1.4	Nanofluids	8
1.4.1	Models for nanofluids	9
1.4.2	Buongiorno model	9
1.5	Fundamentals of heat transfer	9
1.5.1	Modes of heat transfer	9
1.5.2	Specific heat	10
1.5.3	Thermal conductivity	10
1.5.4	Thermal diffusivity	11
1.5.5	Joule heating	11
1.5.6	Viscous dissipation	11
1.6	Peristaltic motion	11

1.6.1	Applications of peristaltic motion	11
1.7	Streamlines	12
1.8	Compliant walls	12
1.9	Mass transfer	12
1.10	Dimensionless numbers	12
1.10.1	Wave number	12
1.10.2	Amplitude ratio	13
1.10.3	Reynolds number	13
1.10.4	Prandtl number	13
1.10.5	Eckert number	13
1.10.6	Brinkman number	14
1.10.7	Hartman number	14
1.10.8	Schmidt number	14
1.10.9	Heat transfer Grashoff number	14
1.10.10	Nanoparticle Grashoff number	15
1.10.11	Brownian motion parameter	15
1.10.12	Thermophoresis parameter	15
1.11	Slip condition	15
1.12	Basic flow equations	16
1.12.1	Continuity equation	16
1.12.2	Equation of motion	16
1.12.3	Energy equation for nanofluids	17
1.12.4	Concentration equation	19
1.13	Solutions methodology	19
1.13.1	Exact method	19
1.13.2	Numerical technique	19
2	Simultaneous effects of slip and wall properties on MHD peristaltic motion of nanofluid with Joule heating	20
2.1	Introduction	20
2.2	Problem geometry	20

2.3	Mathematical modeling	21
2.3.1	Non-dimensionalization	23
2.4	Solution methodology	25
2.4.1	Exact solution for stream function	25
2.4.2	Numerical solution	25
2.5	Graphical results and discussion	25
2.5.1	Velocity distribution	25
2.5.2	Temperature distribution	26
2.5.3	Nanoparticles mass distribution	26
2.5.4	Heat transfer rate	26
3	Slip effect in peristalsis of Jeffrey nanofluid in a channel	38
3.1	Introduction	38
3.2	Modeling	38
3.2.1	Magnetohydrodynamics	39
3.2.2	Flow governing equations	40
3.2.3	Non-dimensional quantities	42
3.2.4	Utilization of stream function	42
3.3	Discussion	44
3.3.1	Velocity profile	44
3.3.2	Temperature profile	45
3.3.3	Nanoparticle concentration profile	46
3.3.4	Heat transfer coefficient	46
3.4	Conclusion	59

Chapter 1

Definitions and equations related to flow analysis

1.1 Introduction

The main purpose of this chapter is to explain some fundamental concepts and laws related to fluid mechanics which are significant in understanding of analysis given in this thesis.

1.2 Basic concepts of fluid

1.2.1 Fluid

A substance capable of changing its shape with position of its particles when shear stress is applied on it. Even less amount of shear force causes deformation. Liquids and gases are considered as fluids because of their flow characteristics.

1.2.2 Fluid mechanics

A vast study of fluid (either at rest or in motion) nature and behavior is studied in a branch of science known as fluid mechanics. It covers an extensive range of applications in engineering, medicine and environmental sciences where the basic laws of mechanics have been employed to deal with fluids.

Classification of fluid flows in fluid mechanics is given below:

Internal flow

When the fluid flow is confined to a solid boundary, the flow is termed as internal flow. Such flow provides favorable models for heat exchange in chemical processes and energy conversion technologies.

External flow

The fluid flow around a submerged body is known as external flow. Some examples include flow over airfoil, sphere, turbine blade and air flow around an aeroplane. All types of flows such as laminar, turbulent, compressible or incompressible flow can occur in both internal and external flow systems.

1.2.3 Newtonian fluid

The fluids for which there exists linear and direct relationship between the shear stress and rate of strain are termed as Newtonian fluids. For such fluids a constant viscosity tensor relates viscous stress and strain rate. Also Newton's law of viscosity is obeyed by such fluids. Mathematically,

$$\text{shear stress} \propto \text{rate of strain} \quad (1.1)$$

$$\tau_{yx} \propto \frac{du}{dy} \quad (1.2)$$

$$\tau_{yx} = \mu \frac{du}{dy} \quad (1.3)$$

where μ is the absolute or dynamic viscosity of fluid, τ_{yx} the shear stress, $\frac{du}{dy}$ the strain rate for one-dimensional flow, x the flow direction and y the direction at which disturbance occur. For two-dimensional flow we have

$$\tau_{yx} = \mu \left(\frac{\partial u}{\partial y} + \frac{\partial v}{\partial x} \right),$$

water, glycerine and air shows Newtonian characteristics.

1.2.4 Non-Newtonian fluid

The fluids for which there exists direct but non-linear relationship between the shear stress applied and rate of strain are termed as non-Newtonian fluids. The viscosity of non-Newtonian fluids depends upon shear rate. Also power law model is obeyed by such fluids. Mathematically,

$$\tau_{yx} = \eta \left(\frac{du}{dy} \right), \quad (1.4)$$

$$\eta = \kappa \left(\frac{du}{dy} \right)^{n-1} \quad n \neq 1, \quad (1.5)$$

where κ denotes the consistency index, n the power law index and η the apparent viscosity. Milk, blood, butter, paint, honey, toothpaste and gels shows non-Newtonian characteristics. Non-Newtonian fluids are divided into three categories:

Time independent fluids

The class of fluids for which shear rate depends only on the shear stress are known as time independent fluids. Wet sand, ketchup and concentrated starch suspension are examples of such fluids.

Time dependent fluids

The class of fluids for which shear rate depends upon shear stress as well as time are known as time dependent fluids. Gelatine, creams and paints are few examples of time dependent fluids.

Viscoelastic fluids

Viscosity (offers resistance to the flow) and elasticity (ability of a material to come back to its original position after the stress is removed) are considered as material properties of a substance. The class of fluids that exhibits both elastic as well as viscous nature are termed as viscoelastic fluids. Amorphous polymers and biopolymers are few examples of such fluids.

1.2.5 Rate type fluid models

The viscoelastic response of the fluids along with property of relaxation and retardation time are classified as rate type fluids. Jeffrey fluids show rheological characteristics of rate type fluids. It is one of the simplest viscoelastic fluid i.e, the internal structure of such materials can sustain stress for some time. Instead of time derivatives, the substantial derivatives are involved in this model. Relaxation/ retardation times are basic advantage of this model.

Relaxation time

Stress forces applied on a system causes disturbance in it. This disturbance results in a deshaped perturbed system. When the forces are removed the disbalanced system comes back to its original shape. As the stresses present in the viscoelastic material donot die out immediately hence the time is required to overcome stress forces, so that the system will come back to its equilibrium position. This time is called relaxation time.

Retardation time

A time required to create stress within a fluid is known as retardation time. Actually it is the time scale through which opposing forces are balanced by applied stresses.

1.2.6 Fluid density

It is the material property that explains the relation between mass and unit volume of a fluid at a particular temperature and pressure. Density has direct relation with pressure while inverse relation with temperature. The mathematical expression for density is

$$\rho_f = \frac{\bar{M}}{v'}, \quad (1.6)$$

where ρ_f denotes the density (measured in $\frac{kg}{m^3}$), \bar{M} the mass (measured in kg) and v' the volume (measured in m^3).

1.2.7 Fluid viscosity

The quality of a fluid that measures the resistance of its particles is known as viscosity. Basically it is a ratio between the stress applied to the resultant strain. Mathematically it can be written as

$$\mu = \frac{\tau_{xy}}{\frac{du}{dy}}, \quad (1.7)$$

where μ denotes the dynamic viscosity (measured in $Pa.sec$ or $\frac{kg}{m.sec}$).

Kinematic viscosity

When the absolute/ dynamic viscosity of the fluid is divided by its density then the viscosity obtained is known as kinematic viscosity. Mathematically it can be written as

$$\nu = \frac{\mu}{\rho_f}. \quad (1.8)$$

It is measured in $\frac{m^2}{sec}$.

1.3 Pressure

The magnitude of force acting perpendicularly to a surface area is known as pressure. Its mathematical description is

$$P = \frac{F}{A}, \quad (1.9)$$

where F is magnitude of force (measured in $\frac{kgm}{sec^2}$) and A is the surface area (measured in m^2).

1.4 Nanofluids

The traditional fluids comprising of nanometer sized particles are named as nanofluids. It is basically suspension of nanoparticles such as metals, carbides, oxides or carbon nanotubes in the base fluid. Water, ethylene glycol and oil are among base fluids. Its major applications cover vivo therapy, surgery, protein engineering, cancer diagnosis and therapy etc.

1.4.1 Models for nanofluids

Several models for nanofluids have been reported in the past including Maxwells model (1904), Hamilton and Crosser's model (1962), Yu and Choi model (2003), Jang and Choi model (2004) and Buongiorno model (2009).

1.4.2 Buongiorno model

Jacopo Buongiorno in 2006 reported that among seven slip mechanisms (inertia, Brownian diffusion, thermophoresis, diffusionphoresis, magnus effect, fluid drainage, and gravity) only Brownian motion and thermophoresis are prominent and responsible for enhancement of thermal conductivity. Buongiorno in 2009 found that thermal conductivity of nanofluids enhances upon enhancement in particle concentration, aspect ratio and reducing base fluid conductivity.

1.5 Fundamentals of heat transfer

Temperature

Temperature is the average kinetic energy of particles in a given sample. It is measured in kelvin K .

Heat

The exchange of energy from one system to another due to temperature difference is known as heat.

1.5.1 Modes of heat transfer

Heat is transferred from one place to another through three modes named as conduction, convection and radiation.

Conduction Particle to particle energy transfer through collision takes place in process of conduction. Its example includes a cold iron skillet placed on a stove and a cube of ice placed into the man's hand etc.

Convection The transfer of energy through the replacement of warmed matter by cold one is termed as convection. Convection is further categorized as forced, natural and mixed convection. Cooling a cup of coffee is an example of convection.

Forced convection When some external agent such as fan or a pump forces the fluid to flow over a surface then such type of convection is known as forced convection.

Natural convection The type of convection in which the density and temperature differences are responsible for the fluid flow is termed as natural convection. So gravity is major agent for such type of convection.

Mixed convection The type of convection in which forced and natural convection occurs simultaneously is called mixed convection.

Radiation The emission of energy in the form of electromagnetic waves from a heated surface is called thermal radiation. Actually the intensity of the radiated energy is governed by the temperature of the heated surface. It is seen that radiative heat transfer uses light that is how the heat from the sun reaches us.

1.5.2 Specific heat

It is the measure of heat energy required to enhance the temperature by one degree celsius.

1.5.3 Thermal conductivity

The extent to which a material can conduct heat is known as thermal conductivity. A good conductor corresponds to high thermal conductivity which depends on temperature gradient. It is measured in $\frac{kgm}{sec^3 K}$.

1.5.4 Thermal diffusivity

It is the relation between ability of a material to transmit heat energy and to store thermal energy is termed as thermal diffusivity. Mathematically,

$$\alpha = \frac{k}{\rho C_p}, \quad (1.10)$$

where C_p is the specific heat, k the thermal conductivity and α the thermal diffusivity. Its unit is $\frac{m^2}{\text{sec}}$.

1.5.5 Joule heating

The loss of kinetic energy of fluid particles in the form of heat is known as Joule heating. The surface temperature of a body directly relates to heat transfer rate in this process.

1.5.6 Viscous dissipation

It is the irreversible process by which the work done on adjacent layers of fluid results in loss of energy is termed as viscous dissipation. The work done is basically against viscous forces.

1.6 Peristaltic motion

The mechanism by which contents of mixture moves ahead under the influence of progressive wave of contraction and expansion is termed as peristalsis. In particular this activity involves mixing and pushing materials through contraction or expansion of the waves propagating along the channel walls in response to pressure.

1.6.1 Applications of peristaltic motion

The peristaltic phenomenon works physiologically in the digestive tract, in the bile duct for transport of bile juice and motion of spermatozoa in cervical canal etc. Also in chemical processes and medical industry this mechanism covers heart lung machine, noxious fluid transport, roller and finger pumps, novel pharmacological delivery systems and in the locomotion of worms etc.

1.7 Streamlines

These are the curves tangential to the instantaneous velocity vector. During fluid flow the orientation of each particle is shown through these imaginary lines. Thus such lines cannot cross each other except at points where the velocity magnitude is zero.

1.8 Compliant walls

Compliance means the ability of the vessels to attain original dimensions after the removal of constricting force. Thus wall compliance refers to the damping, stretching, flexibility and elasticity of the walls. Physiologically such walls play an important role in cardiovascular and respiratory system where the increasing pressure of blood causes the arteries and veins to stretch. Thus the higher compliance deforms easily as compared to the lower compliance blood vessels. Good results are obtained for less channel width i.e. 0.05 or less.

1.9 Mass transfer

The movement of the fluid from one location to another is called mass transfer. In nanofluids mass transfer takes place due to phenomena of diffusion and Brownian motion. Blood purification in the kidneys and liver is an example of mass transfer.

1.10 Dimensionless numbers

1.10.1 Wave number

It is defined as the ratio of half channel width to the wavelength. It basically calculates the number of waves existing at a specified distance. Mathematically, we write

$$\delta = \frac{d_1}{\lambda}, \quad (1.11)$$

where d_1 represents the half channel width and λ the wavelength.

1.10.2 Amplitude ratio

It is the ratio describing the relation between maximum displacement of wave to the half channel width. Mathematically

$$\epsilon = \frac{a}{d_1} \quad (1.12)$$

where a is the wave amplitude.

1.10.3 Reynolds number

It is defined as ratio of inertial to viscous forces. Mathematically, it can be expressed as

$$\text{Re} = \frac{c\rho_f d_1}{\mu}, \quad (1.13)$$

where c corresponds to the wave speed. The Reynolds number determines that either the flow is laminar or turbulent. Low Reynolds number ($Re < 2300$) refers to laminar flow while high Reynolds number ($2300 < Re < 4000$) refers to the turbulent one.

1.10.4 Prandtl number

It can be interpreted as the ratio of momentum diffusivity over thermal diffusivity. Mathematically one can express it as

$$\text{Pr} = \frac{\nu\rho_f C_p}{k}. \quad (1.14)$$

Here C_p is the specific heat, ν the kinematic viscosity and k the thermal conductivity.

1.10.5 Eckert number

The expression for the ratio of kinetic energy to enthalpy is called Eckert number. In mathematical form one can write

$$Ec = \frac{c^2}{C_p \nabla T}, \quad (1.15)$$

where *enthalpy* = *internal energy* + *pressure* \times *volume* and ∇T the temperature difference between the walls.

1.10.6 Brinkman number

It is defined as the ratio of heat produced by viscous dissipation to the heat transferred by molecular conduction. It can be written as the product of Prandtl number and Eckert number.

$$Br = \text{Pr } Ec. \quad (1.16)$$

1.10.7 Hartman number

It is the ratio of magnetic to the viscous force. Mathematically,

$$M = \sqrt{\frac{B_0^2 d_1^2 \sigma}{\mu}}, \quad (1.17)$$

Here B_0 is the magnetic field strength and σ the electrical conductivity.

1.10.8 Schmidt number

It is the ratio of momentum diffusivity to the mass diffusivity.

$$Sc = \frac{\nu}{D_B}, \quad (1.18)$$

in which D_B is the coefficient of mass diffusivity.

1.10.9 Heat transfer Grashoff number

It is the ratio of buoyancy to the viscous forces acting on fluid with reference to change in temperature. Mathematically

$$Gr = \frac{g \alpha^* (T_1 - T_0) d_1^2}{\nu c}. \quad (1.19)$$

In the above expression g is the force of gravity, α^* the thermal expansion coefficient and T_1 and T_0 are the temperatures at the walls.

1.10.10 Nanoparticle Grashoff number

This dimensionless number refers to the ratio of buoyancy to the viscous forces with reference to nanofluid particles. Mathematically

$$Gr = \frac{g\beta^*(C_1 - C_0)d_1^2}{\nu c}, \quad (1.20)$$

where β^* is the concentration expansion coefficient, C_1 and C_0 are the concentration at the walls.

1.10.11 Brownian motion parameter

Thermal behavior of nanofluids is characterized through Brownian motion of nanoparticles. Therefore for nanofluids we define Brownian motion parameter as

$$Nb = \frac{\tau^* D_B (C_1 - C_0)}{\nu}, \quad (1.21)$$

in which τ^* is the ratio of heat capacity of nanomaterial to that of fluid.

1.10.12 Thermophoresis parameter

Temperature difference among nanoparticles can cause diffusion of nanoparticles. This phenomenon is termed as thermophoresis. Thus thermophoresis parameter is expressed as

$$Nt = \frac{\tau^* D_T (T_1 - T_0)}{\nu T_m}. \quad (1.22)$$

Here D_T is the thermophoretic diffusion coefficient.

1.11 Slip condition

This condition was proposed by Navier for the cases of fluid-solid interaction. There are many applications in engineering and biology where no-slip condition is not valid like in artificial heart valves. Slip effects cannot be ignored especially in the cases when hydrodynamic, viscoelastic, chemical and gravitational forces acting on the dispersed particles at the walls are negligible.

Thus slip condition explains the direct relation between fluid-solid velocities and stress at the bounded surface. Mathematically,

$$u - u_w \propto \tau_{xy},$$

$$u - u_w = \pm \beta_1 \tau_{xy}. \quad (1.23)$$

in which u is the fluid velocity, u_w the walls velocity, β_1 the velocity slip parameter, \pm signs correspond to the right and left wall or upper and lower wall respectively.

1.12 Basic flow equations

1.12.1 Continuity equation

Conservation of mass in terms of mass influx and outflux gives the mathematical form of continuity equation as follows:

$$\frac{\partial \rho_f}{\partial t} + \nabla \cdot (\rho_f \mathbf{V}) = 0, \quad (1.24)$$

which is satisfied in the absence of source and sink where t represents the time, $\nabla = \left(\frac{\partial}{\partial x}, \frac{\partial}{\partial y} \right)$ the operator applied on $\mathbf{V} = (u, v)$ the velocity components. For an incompressible fluid the above equation reduces to

$$\nabla \cdot \mathbf{V} = 0. \quad (1.25)$$

1.12.2 Equation of motion

By law of conservation of momentum we mean that the momentum lost by some fluid particles is gained by other fluid particles (either by bulk motion or by molecular motion). Thus total amount of momentum remains constant within a system. Together with surface and body forces the momentum equation takes the form:

$$\rho_f \frac{d\mathbf{V}}{dt} = -\nabla p + \text{div } \boldsymbol{\tau} + \rho_f \mathbf{b}, \quad (1.26)$$

where $\boldsymbol{\tau}$ denotes Cauchy stress tensor , p the pressure which is surface force, \mathbf{b} the body force and $\frac{d}{dt}$ the material time derivative defined for two dimensional system as

$$\frac{d}{dt} = \frac{\partial}{\partial t} + u \frac{\partial}{\partial x} + v \frac{\partial}{\partial y}. \quad (1.27)$$

The above eq. (1.26) infact represents force balance for the flow of fluid.

1.12.3 Energy equation for nanofluids

The energy equation for nanofluids can be expressed as

$$\rho_f C_p \frac{dT}{dt} = -\text{div } q^* + h_p^* \nabla \cdot j_p^*, \quad (1.28)$$

in which h_p^* represents the specific enthalpy of nanoparticles, q^* the heat flux and j_p^* the diffusion mass flux of nanoparticles. Writing q^* from Fourier law of heat conduction as

$$q^* = -k \nabla T + h_p^* j_p^*. \quad (1.29)$$

On substituting value of q^* Eq. (1.28) becomes

$$\begin{aligned} \rho_f C_p \frac{dT}{Dt} &= -\nabla \cdot (-k \nabla T + h_p^* j_p^*) + h_p^* \nabla \cdot j_p^*, \\ &= k \nabla^2 T - \nabla \cdot (h_p^* j_p^*) + h_p^* \nabla \cdot j_p^*, \\ &= k \nabla^2 T - h_p^* \nabla \cdot j_p^* - j_p^* \nabla \cdot h_p^* + h_p^* \nabla \cdot j_p^*, \\ &= k \nabla^2 T - j_p^* \nabla \cdot h_p^*. \end{aligned}$$

Using

$$\nabla \cdot h_p^* = C_p \nabla T, \quad (1.30)$$

we arrive at

$$\rho_f C_p \frac{dT}{Dt} = k \nabla^2 T - C_p j_p^* \cdot \nabla T. \quad (1.31)$$

Splitting the diffusion mass flux for Brownian diffusion and thermophoresis we have

$$j_p^* = j_{p,B}^* + j_{p,T}^*, \quad (1.32)$$

in which

$$j_{p,B}^* = \rho_f D_B \nabla C. \quad (1.33)$$

Defining Brownian motion coefficient as

$$D_B = \frac{k^* T}{3\pi\mu d_p}, \quad (1.34)$$

where k^* is the Boltzmann's constant and d_p the nanoparticles diameter. Also

$$j_{p,T}^* = -\rho_f C V_T, \quad (1.35)$$

where

$$V_T = 0.26 \left(\frac{k}{2k + k_p} \right) \frac{\mu}{\rho_f} \frac{\nabla T}{T}, \quad (1.36)$$

in above expression V_T is the thermophoretic velocity, k_p the thermal conductivity of nanoparticles while k is thermal conductivity of fluid. Writing $D_T = 0.26 \left(\frac{k}{2k + k_p} \right) \frac{\mu C}{\rho_f}$ we get

$$j_{p,T}^* = -\rho_f D_T \frac{\nabla T}{T}, \quad (1.37)$$

From Eqs. (1.33 and 1.35) we have

$$j_p^* = \rho_f D_B \nabla C - \rho_f D_T \frac{\nabla T}{T}. \quad (1.38)$$

Hence the energy equation becomes

$$\rho_f C_p \frac{dT}{dt} = k \nabla^2 T + \rho_f C_p [D_B \nabla C \cdot \nabla T + \rho_f D_T \frac{\nabla T \cdot \nabla T}{T}].$$

In the presence of viscous dissipation and thermal radiation above equation takes the form

$$\rho_f C_p \frac{dT}{dt} = k \nabla^2 T + \rho_f C_p [D_B \nabla C \cdot \nabla T + \rho_f D_T \frac{\nabla T \cdot \nabla T}{T}] + \tau \cdot L + \nabla \cdot q_r. \quad (1.39)$$

where q_r is the radiative heat flux.

1.12.4 Concentration equation

By using Fick's law the concentration of nanoparticles involving diffusion of mass can be expressed as

$$\left(\frac{\partial}{\partial t} + \mathbf{V} \cdot \nabla \right) C = -\frac{1}{\rho_f} \nabla \cdot j_p^*,$$

Using Eq. (1.38) in above equation we have

$$\left(\frac{\partial}{\partial t} + \mathbf{V} \cdot \nabla \right) C = D_B \nabla^2 C + \frac{D_T}{T} \nabla^2 T. \quad (1.40)$$

where C and T are the fluid concentration and temperature respectively.

1.13 Solutions methodology

1.13.1 Exact method

The exact solutions for linear boundary value problems can be computed through *DSolve* command in Mathematica.

1.13.2 Numerical technique

Numerical technique involves the graphical results obtained through *NDSolve* command in Mathematica. It gives the approximated results with accuracy controlled upto desired iterations.

Chapter 2

Simultaneous effects of slip and wall properties on MHD peristaltic motion of nanofluid with Joule heating

2.1 Introduction

Peristalsis of magnetohydrodynamic (MHD) nanofluid in a channel with compliant walls is discussed here. Joule heating, viscous dissipation and partial slip effects are considered in the present analysis. System of equations is simplified through long wavelength and low Reynolds number approximation. Solutions for stream function, temperature and concentration are obtained through suitable approach and are thus used to plot graphs. The physical interpretation of graphical results is presented in the last section. This chapter provides the detailed review of a research article by Hayat et al. [13].

2.2 Problem geometry

Peristaltic transport of an incompressible nanofluid is considered in a bounded channel of uniform thickness $2d_1$ in such a way that $x - axis$ is along channel and $y - axis$ is transverse to it.

Here T_0 , T_1 and C_0 , C_1 represent the temperature and concentration at lower and upper walls respectively. Viscous dissipation effects are retained in the problem. The problem is proceeded further by using slip conditions for velocity, temperature and concentration. A uniform magnetic field B_0 is applied in y -direction whereas induced magnetic field is considered absent due to low magnetic Reynolds number. The walls shape can be expressed as

$$y = \pm\eta(x, t) = \pm \left[d_1 + a \sin \frac{2\pi}{\lambda}(x - ct) \right], \quad (2.1)$$

where c is the speed of sinusoidal wave having amplitude a and wavelength λ propagating along the channel in time t . The physical model of the present problem is shown in Fig. 2.1.

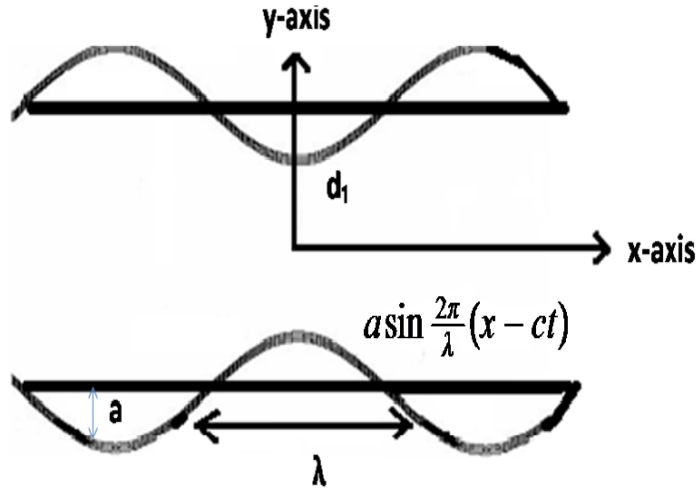


Fig. 2.1. Flow geometry.

2.3 Mathematical modeling

For incompressible viscous fluid the Cauchy stress tensor (τ) is expressed as

$$\tau = -p\mathbf{I} + \mu\dot{\mathbf{A}}_1, \quad (2.2)$$

in which p is the pressure, \mathbf{I} the identity tensor and $\dot{\mathbf{A}}_1$ the first Rivlin Ericksen tensor given by

$$\dot{\mathbf{A}}_1 = (\nabla \mathbf{V}) + (\nabla \mathbf{V})^t, \quad (2.3)$$

with \mathbf{V} and ∇ in two dimensional flows as follows:

$$\mathbf{V} = (u, v, 0),$$

$$\nabla = \left(\frac{\partial}{\partial x}, \frac{\partial}{\partial y}, 0 \right)$$

Hence we obtain

$$\dot{\mathbf{A}}_1 = \begin{bmatrix} 2\frac{\partial u}{\partial x} & \frac{\partial u}{\partial y} + \frac{\partial v}{\partial x} & 0 \\ \frac{\partial u}{\partial y} + \frac{\partial v}{\partial x} & 2\frac{\partial v}{\partial y} & 0 \\ 0 & 0 & 0 \end{bmatrix}. \quad (2.4)$$

The flow is governed through following equations

$$\frac{\partial u}{\partial x} + \frac{\partial v}{\partial y} = 0, \quad (2.5)$$

$$\left(\frac{\partial u}{\partial t} + u \frac{\partial u}{\partial x} + v \frac{\partial u}{\partial y} \right) = -\frac{1}{\rho_f} \frac{\partial p}{\partial x} + \nu \left(\frac{\partial^2 u}{\partial x^2} + \frac{\partial^2 u}{\partial y^2} \right) - \frac{\sigma B_0^2 u}{\rho_f}, \quad (2.6)$$

$$\frac{\partial v}{\partial t} + u \frac{\partial v}{\partial x} + v \frac{\partial v}{\partial y} = -\frac{1}{\rho_f} \frac{\partial p}{\partial y} + \nu \left(\frac{\partial^2 v}{\partial x^2} + \frac{\partial^2 v}{\partial y^2} \right), \quad (2.7)$$

$$\begin{aligned} \frac{\partial T}{\partial t} + u \frac{\partial T}{\partial x} + v \frac{\partial T}{\partial y} &= \alpha \left(\frac{\partial^2 T}{\partial x^2} + \frac{\partial^2 T}{\partial y^2} \right) + \frac{\nu}{C_p} \left[4 \left(\frac{\partial u}{\partial x} \right)^2 + \left(\frac{\partial u}{\partial y} + \frac{\partial v}{\partial x} \right)^2 \right] + \frac{\sigma B_0^2 u^2}{\rho_f c_f} \\ &+ \tau^* \left[D_B \left(\frac{\partial C}{\partial x} \frac{\partial T}{\partial x} + \frac{\partial C}{\partial y} \frac{\partial T}{\partial y} \right) + \frac{D_T}{T_m} \left\{ \left(\frac{\partial T}{\partial x} \right)^2 + \left(\frac{\partial T}{\partial y} \right)^2 \right\} \right], \end{aligned} \quad (2.8)$$

$$\frac{\partial C}{\partial t} + u \frac{\partial C}{\partial x} + v \frac{\partial C}{\partial y} = D_B \left(\frac{\partial^2 C}{\partial x^2} + \frac{\partial^2 C}{\partial y^2} \right) + \frac{D_T}{T_m} \left(\frac{\partial^2 T}{\partial x^2} + \frac{\partial^2 T}{\partial y^2} \right). \quad (2.9)$$

In which we have considered mean temperature T_m because the flow is confined to the flexible boundaries. The relevant boundary conditions

$$u \pm \beta_1 \left(\frac{\partial u}{\partial y} + \frac{\partial v}{\partial x} \right) = 0, \quad \text{at } y = \pm \eta, \quad (2.10)$$

$$T \pm \beta_2 \frac{\partial T}{\partial y} = \left(\frac{T_1}{T_0} \right), \quad C \pm \beta_3 \frac{\partial C}{\partial y} = \left(\frac{C_1}{C_0} \right), \quad \text{at } y = \pm \eta, \quad (2.11)$$

and compliant wall conditions as

$$\left[-\tau_1 \frac{\partial^3}{\partial x^3} + m_1 \frac{\partial^3}{\partial x \partial t^2} + d \frac{\partial^2}{\partial x \partial t} \right] \eta = \mu \left(\frac{\partial^2 u}{\partial x^2} + \frac{\partial^2 u}{\partial y^2} \right) - \rho_f \left(\frac{\partial u}{\partial t} + u \frac{\partial u}{\partial x} + v \frac{\partial u}{\partial y} \right) - \sigma B_0^2 u, \quad (2.12)$$

where ρ_f is the nanofluid density, ν the kinematic viscosity, α the thermal diffusivity, σ the thermal conductivity, D_B the Brownian motion coefficient, D_T the thermophoretic diffusion coefficient and $\tau^* = \frac{(\rho c)_p}{(\rho c)_f}$ the ratio of effective heat capacity of nanoparticle material to heat capacity of fluid, τ_1 the elastic tension, m_1 the mass per unit area, d the coefficient of viscous damping, $\beta_1, \beta_2, \beta_3$ the velocity, thermal and concentration slip parameters respectively, T_m the mean temperature, T and C the temperature and concentration of fluid and μ the fluid dynamic viscosity.

2.3.1 Non-dimensionalization

Defining the following non-dimensional quantities:

$$\begin{aligned} u^* &= \frac{u}{c}, \quad v^* = \frac{v}{c}, \quad x^* = \frac{x}{\lambda}, \quad y^* = \frac{y}{d_1}, \quad \beta_i^* = \frac{\beta_i}{d_1} \quad (i = 1, 2, 3), \quad t^* = \frac{ct}{\lambda}, \\ \eta^* &= \frac{\eta}{d_1}, \quad p^* = \frac{d_1^2 p}{c \lambda \mu}, \quad \theta = \frac{T - T_0}{T_1 - T_0}, \quad \phi = \frac{C - C_0}{C_1 - C_0}. \end{aligned} \quad (2.13)$$

Omitting asterisks from Eqs.(2.6) – (2.12) and by the definition of stream function $\psi(x, y, t)$ writing

$$u = \frac{\partial \psi}{\partial y}, \quad v = -\delta \frac{\partial \psi}{\partial x},$$

the above equations become

$$\text{Re} \left[\delta \frac{\partial^2 \psi}{\partial t \partial y} + \delta \frac{\partial \psi}{\partial y} \frac{\partial^2 \psi}{\partial x \partial y} - \delta \frac{\partial \psi}{\partial x} \frac{\partial^2 \psi}{\partial y^2} \right] = -\frac{\partial p}{\partial x} + \left(\delta^2 \frac{\partial^2 u}{\partial x^2} + \frac{\partial^2 u}{\partial y^2} \right) - M^2 u, \quad (2.14)$$

$$\text{Re} \delta \left[-\delta^2 \frac{\partial^2 \psi}{\partial x \partial t} - \delta^2 \frac{\partial \psi}{\partial y} \frac{\partial^2 \psi}{\partial x^2} - \delta^2 \frac{\partial^2 \psi}{\partial x \partial y} \right] = -\frac{\partial p}{\partial y} + \delta \left(\delta^2 \frac{\partial^2 v}{\partial x^2} + \frac{\partial^2 v}{\partial y^2} \right), \quad (2.15)$$

$$\begin{aligned}
\text{Re} \left[\delta \frac{\partial \theta}{\partial t} + u \delta \frac{\partial \theta}{\partial x} + v \frac{\partial \theta}{\partial y} \right] &= Ec \left[4 \left(\delta \frac{\partial^2 \psi}{\partial x \partial y} \right)^2 + \left(-\delta^2 \frac{\partial^2 \psi}{\partial x^2} + \frac{\partial^2 \psi}{\partial y^2} \right)^2 + M^2 \left(\frac{\partial \psi}{\partial y} \right)^2 \right] \\
&+ Nb \left[\delta^2 \frac{\partial \phi}{\partial x} \frac{\partial \theta}{\partial x} + \frac{\partial \phi}{\partial y} \frac{\partial \theta}{\partial y} \right] + Nt \left[\left(\delta \frac{\partial \theta}{\partial x} \right)^2 + \left(\frac{\partial \theta}{\partial y} \right)^2 \right] \\
&+ \frac{1}{\text{Pr}} \left(\delta^2 \frac{\partial^2 \theta}{\partial x^2} + \frac{\partial^2 \theta}{\partial y^2} \right), \tag{2.16}
\end{aligned}$$

$$\text{Re} Sc \left[\delta \frac{\partial \phi}{\partial t} + \delta \frac{\partial \psi}{\partial y} \frac{\partial \phi}{\partial x} - \delta \frac{\partial \psi}{\partial x} \frac{\partial \phi}{\partial y} \right] = \left(\delta^2 \frac{\partial^2 \phi}{\partial x^2} + \frac{\partial^2 \phi}{\partial y^2} \right) + \frac{Nt}{Nb} \left(\delta^2 \frac{\partial^2 \theta}{\partial x^2} + \frac{\partial^2 \theta}{\partial y^2} \right), \tag{2.17}$$

along with the boundary conditions as

$$\frac{\partial \psi}{\partial y} \pm \beta_1 \left(\frac{\partial^2 \psi}{\partial y^2} - \delta^2 \frac{\partial^2 \psi}{\partial x^2} \right) = 0, \quad \text{at } y = \pm \eta, \tag{2.18}$$

$$\theta \pm \beta_2 \frac{\partial \theta}{\partial y} = \begin{pmatrix} 1 \\ 0 \end{pmatrix}, \quad \phi \pm \beta_3 \frac{\partial \phi}{\partial y} = \begin{pmatrix} 1 \\ 0 \end{pmatrix}, \quad \text{at } y = \pm \eta, \tag{2.19}$$

$$\begin{aligned}
\left[E_1 \frac{\partial^3}{\partial x^3} + E_2 \frac{\partial^3}{\partial x \partial t^2} + E_3 \frac{\partial^2}{\partial x \partial t} \right] \eta &= + \left[\delta^2 \frac{\partial^3 \psi}{\partial y \partial x^2} + \frac{\partial^3 \psi}{\partial y^3} \right] - M^2 \frac{\partial \psi}{\partial y} \\
- \text{Re} \left[\delta \frac{\partial^2 \psi}{\partial t \partial y} + \delta \frac{\partial \psi}{\partial y} \frac{\partial^2 \psi}{\partial x \partial y} - \delta \frac{\partial \psi}{\partial x} \frac{\partial^2 \psi}{\partial x \partial y} \right], \quad \text{at } y = \pm \eta, \tag{2.20}
\end{aligned}$$

by long wavelength and low Reynolds number approximation we obtain

$$\frac{\partial^4 \psi}{\partial y^4} - M^2 \frac{\partial^2 \psi}{\partial y^2} = 0, \tag{2.21}$$

$$\frac{1}{\text{Pr}} \frac{\partial^2 \theta}{\partial y^2} + Nb \frac{\partial \theta}{\partial y} \frac{\partial \phi}{\partial y} + Nt \left(\frac{\partial \theta}{\partial y} \right)^2 + Ec \left[\left(\frac{\partial^2 \psi}{\partial y^2} \right)^2 + M^2 \left(\frac{\partial \psi}{\partial y} \right)^2 \right] = 0, \tag{2.22}$$

$$\frac{\partial^2 \phi}{\partial y^2} + \frac{Nt}{Nb} \left(\frac{\partial^2 \theta}{\partial y^2} \right) = 0, \tag{2.23}$$

with boundary conditions

$$\frac{\partial \psi}{\partial y} \pm \beta_1 \left(\frac{\partial^2 \psi}{\partial y^2} \right) = 0, \quad \theta \pm \beta_2 \frac{\partial \theta}{\partial y} = \begin{pmatrix} 1 \\ 0 \end{pmatrix}, \quad \phi \pm \beta_3 \frac{\partial \phi}{\partial y} = \begin{pmatrix} 1 \\ 0 \end{pmatrix}, \quad \text{at } y = \pm \eta, \tag{2.24}$$

$$\left[E_1 \frac{\partial^3}{\partial x^3} + E_2 \frac{\partial^3}{\partial x \partial t^2} + E_3 \frac{\partial^2}{\partial x \partial t} \right] \eta = \frac{\partial^3 \psi}{\partial y^3} - M^2 \frac{\partial \psi}{\partial y}, \quad \text{at } y = \pm \eta, \tag{2.25}$$

where $\epsilon = \frac{a}{d_1}$ is the amplitude ratio, $\delta = \frac{d_1}{\lambda}$ the wave number, $Nb = \frac{\tau^* D_B (C_1 - C_0)}{\nu}$ and $Nt = \frac{\tau^* D_T (T_1 - T_0)}{T_m \nu}$ the Brownian motion and thermophoresis parameters respectively, $Re = \frac{c \rho d_1}{\mu}$ the Reynolds number, $Sc = \frac{\nu}{D_B}$ the Schmidt number, $M = \sqrt{\frac{\sigma}{\mu}} B_0 d_1$ the Hartman number, $Ec = \frac{c^2}{C_p (T_1 - T_0)}$ the Eckert number, $Pr = \frac{\nu \rho C_p}{k}$ the Prandtl number, $E_1 = -\frac{\tau_1 d_1^3}{\lambda^3 \mu c}$, $E_2 = \frac{m_1 d_1^3 c}{\lambda^3 \mu}$ and $E_3 = \frac{d d_1^3}{\lambda^2 \mu}$ the wall parameters.

2.4 Solution methodology

2.4.1 Exact solution for stream function

Exact solution of Eq. (2.21) with boundary conditions (2.24) and (2.25) is given as

$$\psi = \frac{8c\pi^3 \left[\frac{E_3}{2\pi} \sin 2\pi(x-t) - (E_1 + E_2) \cos 2\pi(x-t) \right]}{M^2} \left[\frac{\sinh My}{M(\cos M\eta + M\beta_1 \sinh M\eta)} - y \right]. \quad (2.26)$$

2.4.2 Numerical solution

The exact solutions for (2.22) – (2.23) seems difficult to attain since these equations are non-linear. Hence solutions for temperature and concentration are obtained by substituting ψ in Eqs. (2.22 and 2.23) with boundary conditions given in Eq. (2.24) using the built-in command *NDSolve* of Mathematica.

2.5 Graphical results and discussion

To discuss the influence of various parameters on velocity, temperature, concentration and heat transfer rate towards different parameters is main interest here. Thus their physical illustration is made in following subsections.

2.5.1 Velocity distribution

Fig. 2.2 shows the plot of velocity for various values of velocity slip parameter β_1 . It is due to less resistance caused by slip which enhances the velocity profile (see Fig. 2.2). Similar behavior is observed for amplitude ratio parameter ϵ (see Fig. 2.3). As electromagnetic force exhibits

retarding nature that is why velocity profile reduces upon enhancement in Hartman number M (see Fig. 2.4). It is observed from Fig. 2.5 that velocity enhances for increasing values of wall elasticity parameters E_1 and E_2 while it reduces under wall damping effect E_3 . Moreover it is noticed that graph is parabolic in shape and has maximum magnitude near the center of channel (see Fig. 2.5).

2.5.2 Temperature distribution

Fig. 2.6 displays the combined sketch of Brownian motion parameter Nb and thermophoresis parameter Nt on temperature profile. It is notified that both the mechanisms causes increase in temperature of the nanofluid (see Fig. 2.6). An increase in temperature is observed for increasing values of Prandtl number Pr (see Fig. 2.7). Moreover strong viscous dissipation effects enhance the temperature that is why Eckert number Ec is an increasing function of temperature (see Fig. 2.8). Fig. 2.9 portrays the graph of temperature for variation in wall parameters E_1 , E_2 and E_3 . It is observed that temperature is an increasing function of E_1 and E_2 while it is decreasing function of E_3 (see Fig. 2.9). Also temperature is an increasing function of amplitude ratio ϵ and thermal slip parameter β_2 (see Figs. 2.10 and 2.11). Fig. 2.12 shows that Hartman number M causes decay in temperature.

2.5.3 Nanoparticles mass distribution

An active motion of nanoparticles from walls to the fluid increases mass flux hence concentration profile increases for increasing values of Brownian motion parameter Nb (see Fig. 2.13). Figs. 2.14 and 2.15 shows that concentration is a decreasing function of corresponding slip parameter β_3 and increasing function of Hartman number M (see Figs. 2.14 and 2.15). Fig. 2.16 depicts that elasticity of walls E_1 and E_2 cause a decay in concentration while damping E_3 enhances it (see Fig. 2.16).

2.5.4 Heat transfer rate

Various illustrations for heat transfer rate Z have been made in the presence ($Ec = 1$) and absence ($Ec = 0$) of viscous dissipation effects. It is noticed that in the presence of viscous dissipation heat transfer is not smooth. Heat transfer Z is more for increasing values of Prandtl

number Pr in presence of viscous dissipation (see Fig. 2.17 (a)) however less heat transfer occurs in absence of viscous dissipation (see Fig. 2.17 (b)). Also it is noticed from Fig. 2.18 (a) that Z is decreasing function of Hartman number M whereas no prominent heat transfer is observed for M when viscous dissipation is neglected (see Fig. 2.18 (b)). Also heat transfer rate reduces for Brownian motion parameter Nb and thermophoresis parameter Nt for both cases (see Figs. 2.19 (a) and (b)).

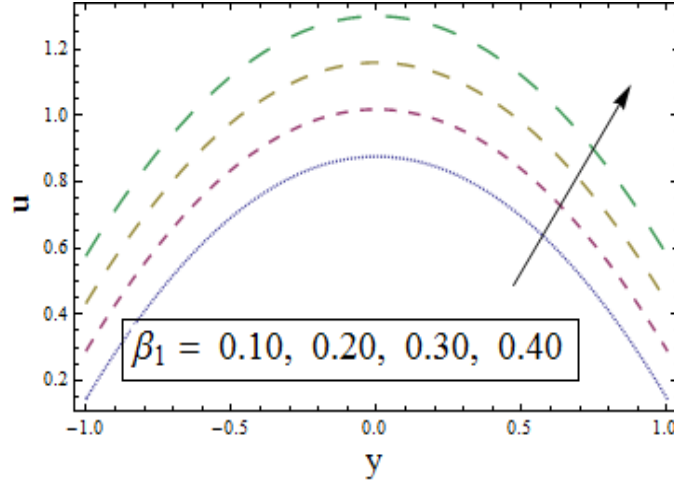


Fig. 2.2.

Fig. 2.2. Sketch of u for different values of β_1 when $x = 0.1$, $\epsilon = 0.2$, $t = 0.1$, $M = 0.1$, $E_1 = E_2 = 0.02$, $E_3 = 0.01$.

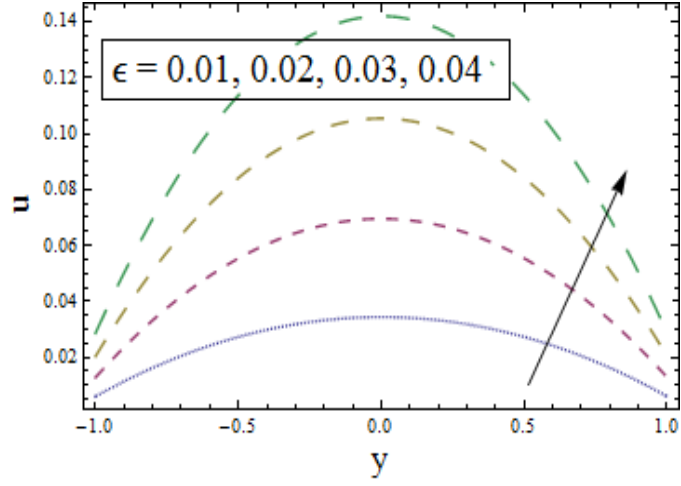


Fig. 2.3.

Fig. 2.3. Sketch of u for different values of ϵ when $x = 0.1$, $t = 0.1$, $\beta_1 = 0.1$, $M = 0.3$, $E_1 = E_2 = 0.02$, $E_3 = 0.01$.

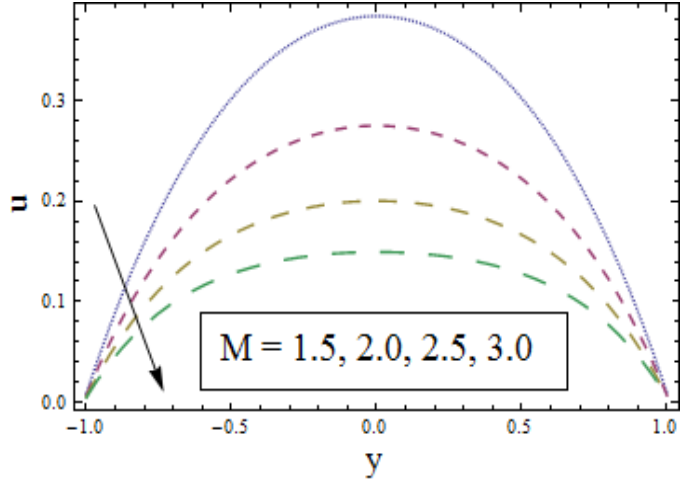


Fig. 2.4.

Fig. 2.4. Sketch of u for different values of M when $\epsilon = 0.2$, $x = 0.1$, $t = 0.1$, $\beta_1 = 0.1$, $E_1 = E_2 = 0.02$, $E_3 = 0.01$.

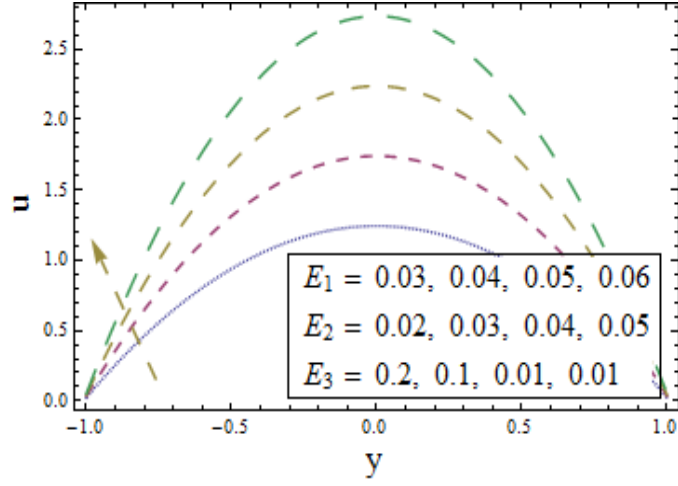


Fig. 2.5.

Fig. 2.5. Sketch of u for different values of E_1, E_2, E_3 when $x = 0.1, \epsilon = 0.2, t = 0.1, \beta_1 = 0.1, M = 0.3$.

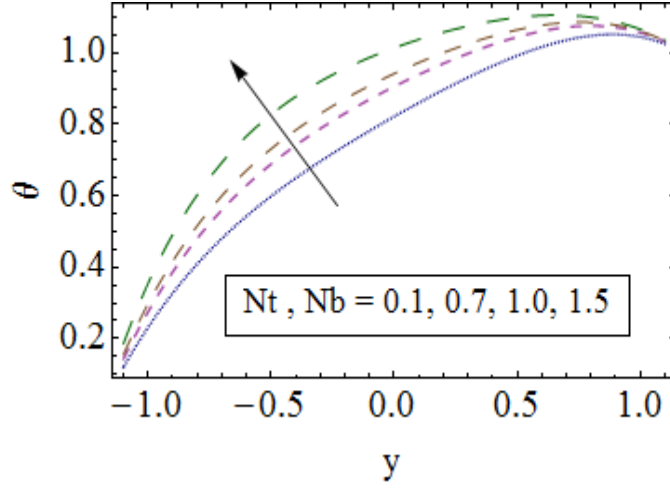


Fig. 2.6.

Fig. 2.6. Sketch of θ for different values of Nb, Nt when $x = 0.1, \epsilon = 0.2, t = 0.1, Pr = 0.6, \beta_1 = \beta_3 = \beta_2 = 0.1, M = 0.3, Ec = 1.8, E_1 = E_2 = 0.02, E_3 = 0.01$.

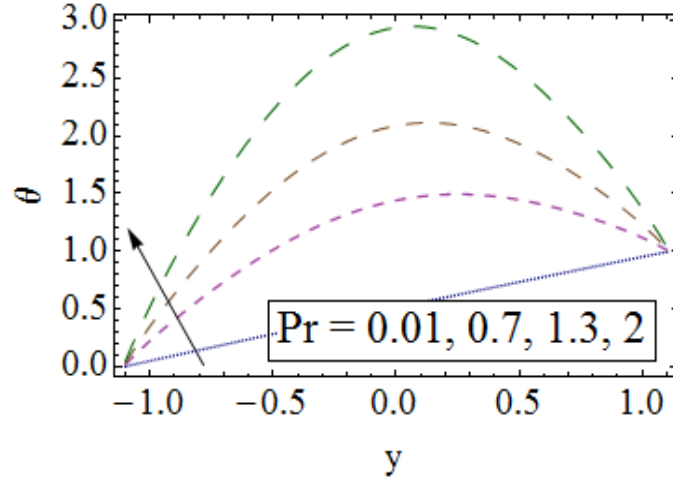


Fig. 2.7.

Fig. 2.7. Sketch of θ for different values of Pr when $x = 0.1$, $\epsilon = 0.2$, $t = 0.1$, $Nb = 0.6$, $Nt = 0.5$, $\beta_1 = \beta_3 = \beta_2 = 0.1$, $M = 0.3$, $Ec = 1.8$, $E_1 = E_2 = 0.02$, $E_3 = 0.01$.

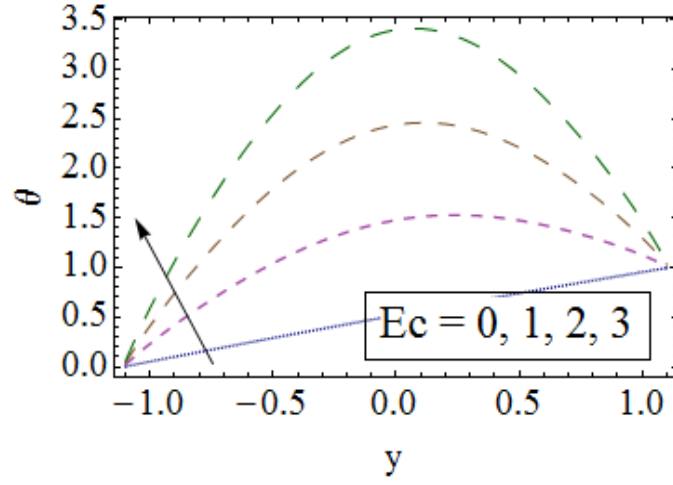


Fig. 2.8.

Fig. 2.8. Sketch of θ for different values of Ec when $x = 0.2$, $\epsilon = 0.2$, $t = 0.1$, $Nb = 0.6$, $Nt = 0.5$, $\beta_1 = \beta_3 = \beta_2 = 0.1$, $M = 0.3$, $Pr = 1.8$, $E_1 = E_2 = 0.02$, $E_3 = 0.01$.

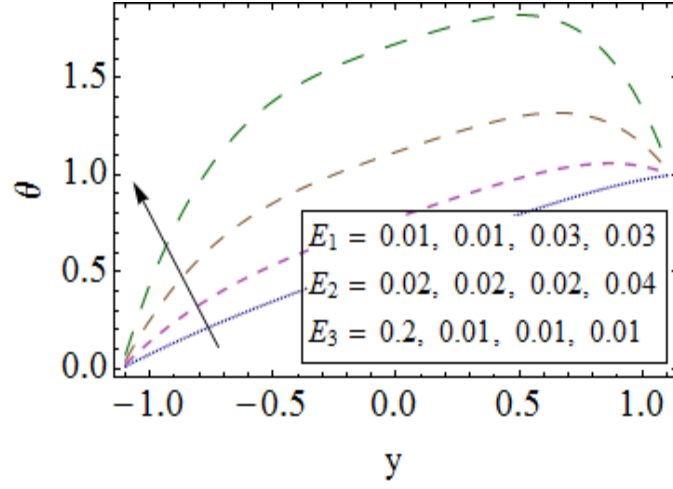


Fig. 2.9.

Fig. 2.9. Sketch of θ for different E_1, E_2, E_3 values of when $x = 0.1$, $\epsilon = 0.2$, $t = 0.1$, $Nb = 0.6$, $Nt = 0.5$, $\beta_1 = \beta_3 = \beta_2 = 0.1$, $M = 0.3$, $Pr = 1.8$, $Ec = 1.2$.

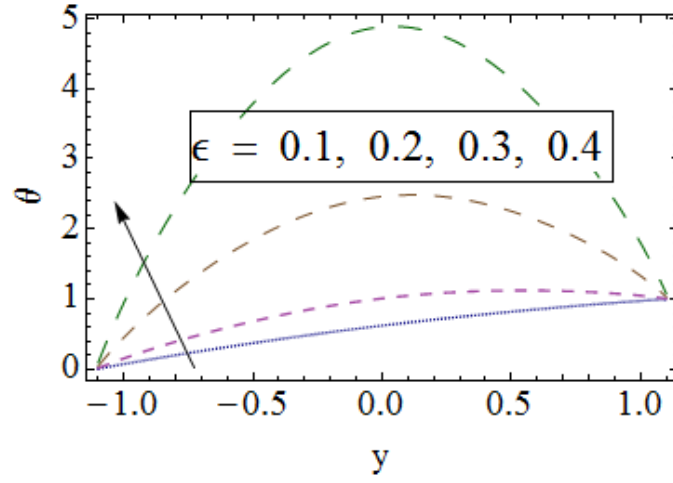


Fig. 2.10.

Fig. 2.10. Sketch of θ for different values of ϵ when $x = 0.1$, $t = 0.1$, $Nb = 0.6$, $Nt = 0.5$, $\beta_1 = \beta_3 = \beta_2 = 0.1$, $M = 0.3$, $Pr = 1.8$, $E_1 = E_2 = 0.05$, $E_3 = 0.01$.

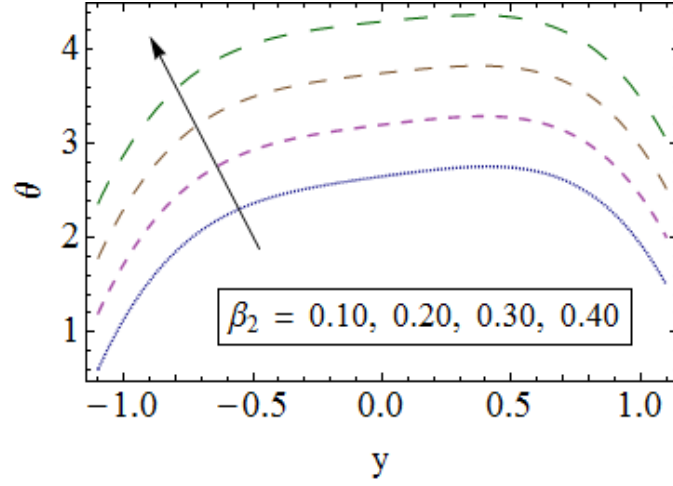


Fig. 2.11.

Fig. 2.11. Sketch of θ for different values of β_2 when $x = 0.1$, $\epsilon = 0.2$, $t = 0.1$, $Nb = 0.6$, $Nt = 0.5$, $\beta_1 = \beta_3 = 0.1$, $M = 0.3$, $Pr = 1.8$, $Ec = 1$, $E_1 = 0.05$, $E_2 = 0.05$, $E_3 = 0.01$.

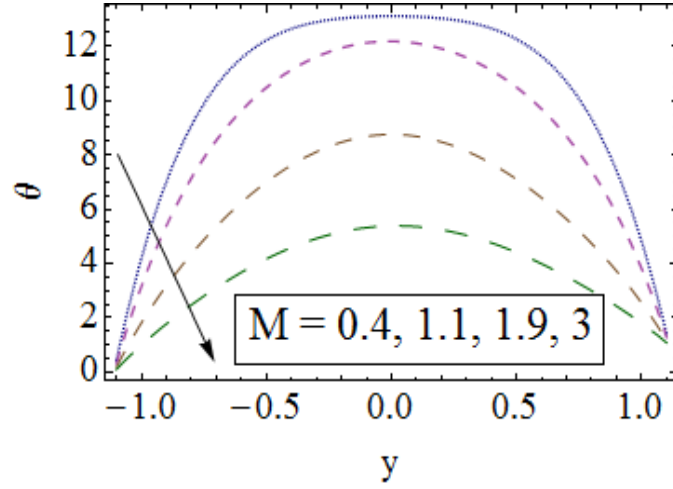


Fig. 2.12.

Fig. 2.12. Sketch of θ for different values of M when $x = 0.1$, $\epsilon = 0.2$, $t = 0.1$, $Nb = 0.6$, $Nt = 0.5$, $\beta_1 = \beta_2 = \beta_3 = 0.1$, $Pr = 1.8$, $Ec = 1$, $E_1 = 0.05$, $E_2 = 0.05$, $E_3 = 0.01$.

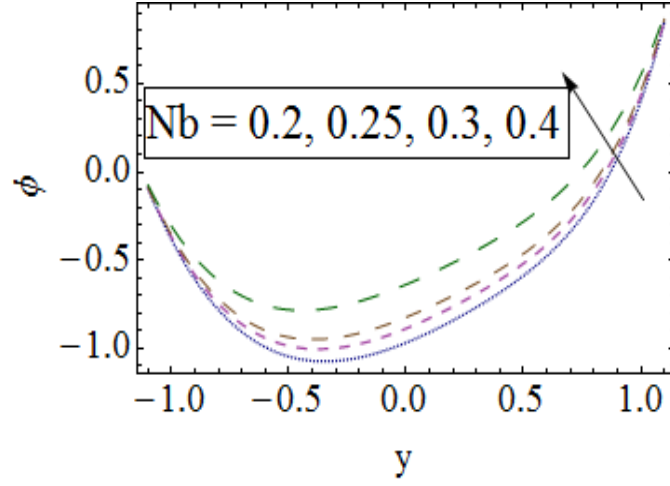


Fig. 2.13.

Fig. 2.13. Sketch of ϕ for different values of Nb when $x = 0.1$, $\epsilon = 0.2$, $t = 0.1$, $Nt = 0.5$, $\beta_1 = \beta_2 = \beta_3 = 0.1$, $M = 0.2$, $Pr = 1.8$, $Ec = 1$, $E_1 = E_2 = 0.05$, $E_3 = 0.01$.

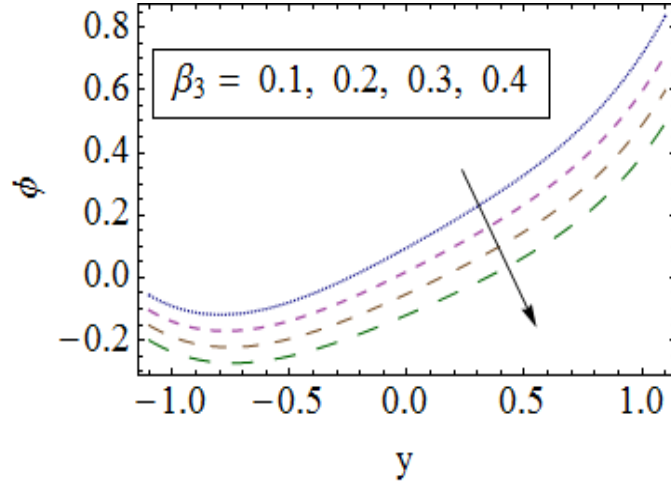


Fig. 2.14.

Fig. 2.14. Sketch of ϕ for different values of β_3 when $x = 0.1$, $\epsilon = 0.2$, $t = 0.1$, $Nb = 0.6$, $Nt = 0.5$, $\beta_1 = \beta_2 = 0.1$, $M = 0.2$, $Ec = 1$, $Pr = 1.8$, $E_1 = E_2 = 0.05$, $E_3 = 0.01$.

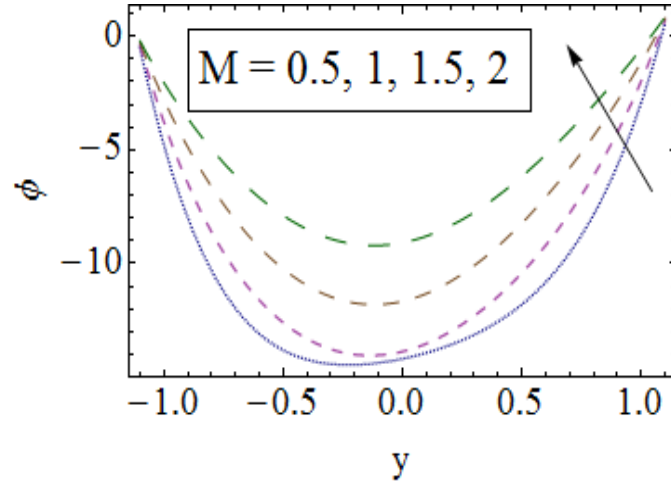


Fig. 2.15.

Fig. 2.15. Sketch of ϕ for different values of M when $x = 0.1$, $\epsilon = 0.2$, $t = 0.1$, $Nb = 0.6$, $Nt = 0.5$, $\beta_1 = \beta_2 = \beta_3 = 0.1$, $Pr = 1.8$, $Ec = 1$, $E_1 = E_2 = 0.05$, $E_3 = 0.01$.

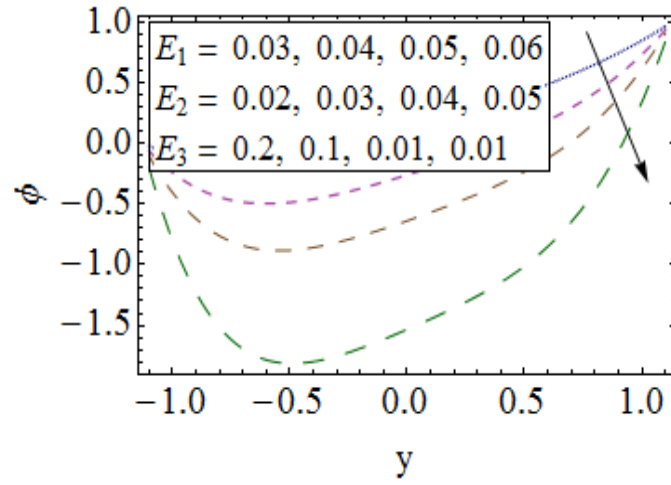


Fig. 2.16.

Fig. 2.16. Sketch of ϕ for different values of E_1, E_2, E_3 when $\epsilon = 0.2$, $x = 0.1$, $t = 0.1$, $M = 0.2$, $Nb = 0.6$, $Nt = 0.5$, $\beta_1 = \beta_2 = \beta_3 = 0.1$, $Pr = 1.8$, $Ec = 1$.

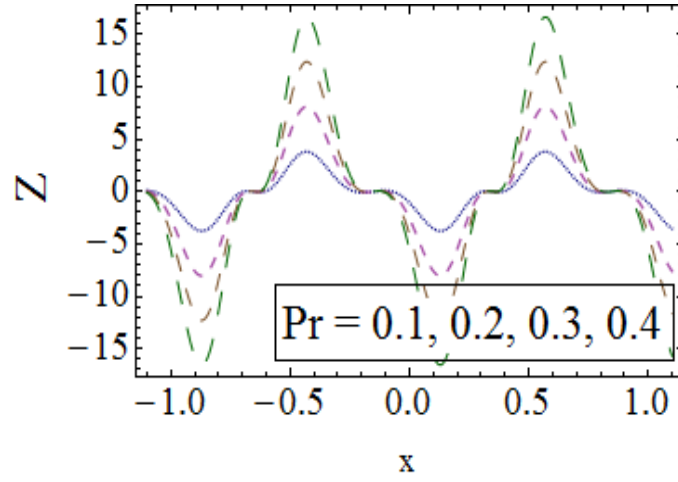


Fig. 2.17 (a).

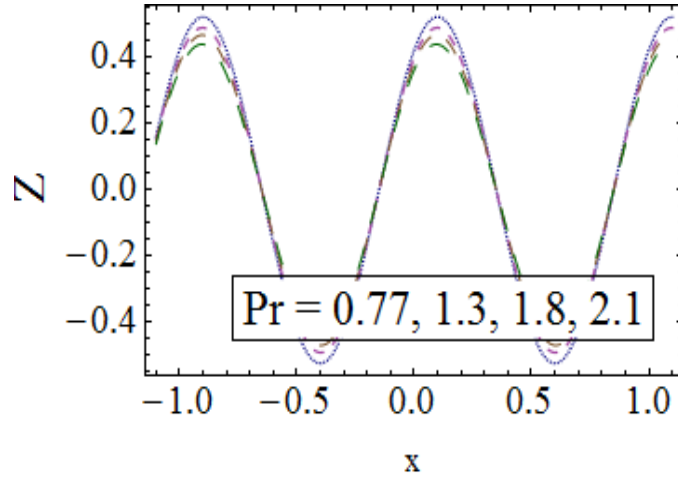


Fig. 2.17 (b).

Fig. 2.17. Sketch of Z for different values of Pr when $\epsilon = 0.2$, $t = 0.1$, $M = 0.2$, $Nb = 0.6$, $Nt = 0.5$, $\beta_1 = \beta_2 = \beta_3 = 0.1$, $E_1 = 0.01$, $E_3 = 0.01$, $E_2 = 0.2$, (a) $Ec = 1$, (b) $Ec = 0$.

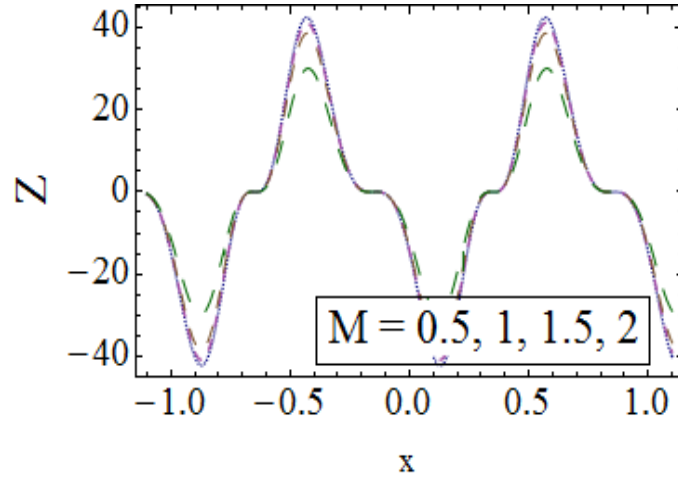


Fig. 2.18 (a).

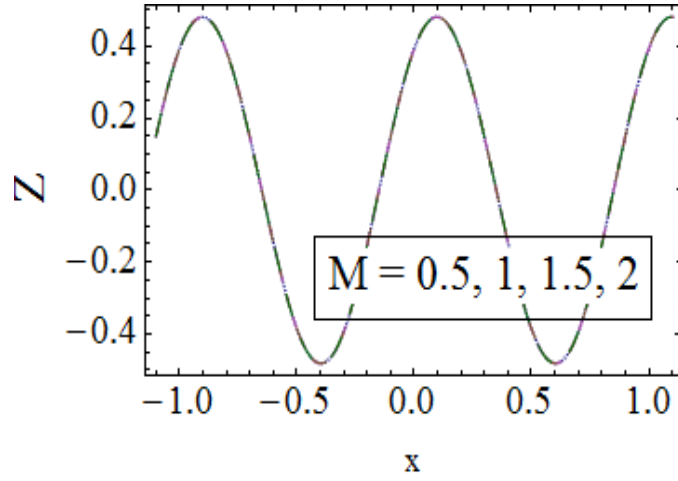


Fig. 2.18 (b).

Fig. 2.18. Sketch of Z for different values of M when $\epsilon = 0.2$, $t = 0.1$, $Pr = 1$, $Nb = 0.6$, $Nt = 0.5$, $\beta_1 = \beta_2 = \beta_3 = 0.1$, $E_1 = 0.1$, $E_3 = 0.01$, $E_2 = 0.2$, (a) $Ec = 1$, (b) $Ec = 0$.

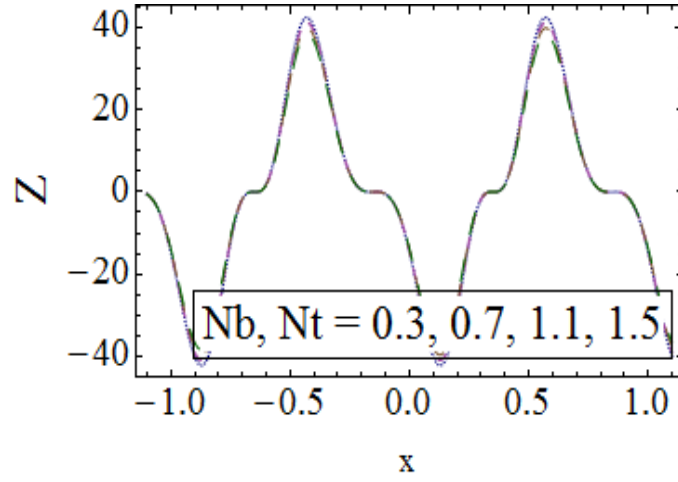


Fig. 2.19 (a).

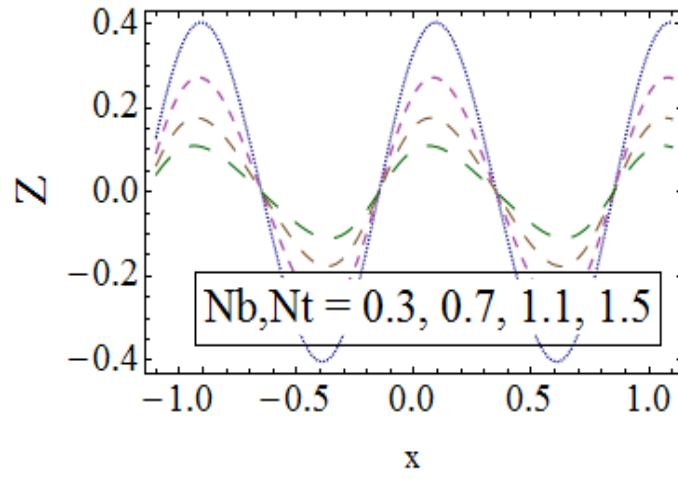


Fig. 2.19 (b).

Fig. 2.19. Sketch of Z for different values of Nb, Nt when $\epsilon = 0.2$, $t = 0.1$, $Pr = 1$, $M = 2$, $\beta_1 = \beta_2 = \beta_3 = 0.1$, $E_1 = 0.1$, $E_3 = 0.01$, $E_2 = 0.2$, (a) $Ec = 1$, (b) $Ec = 0$.

Chapter 3

Slip effect in peristalsis of Jeffrey nanofluid in a channel

3.1 Introduction

Influence of mixed convection on peristalsis of Jeffrey nanofluid in a channel with compliant boundaries is addressed here. This investigation includes the thermal radiation and Joule heating effects. Whole analysis is performed for velocity, thermal and concentration slip conditions. Related problems through long wavelength and low Reynolds number are examined for stream function, temperature and concentration. Impacts of Joule heating, Grashoff number, Hartman number, thermal radiation, slip parameters, thermophoresis and Brownian motion parameter are explored in detail.

3.2 Modeling

We consider two-dimensional flow of an incompressible Jeffrey nanofluid in a symmetric channel of uniform thickness $2d_1$. The sinusoidal wave is propagating along the walls of the channel with wavelength λ and constant speed c . The slip conditions for velocity, temperature and concentration are considered. Here x and y describe the axial and transverse directions. Let $y = -\eta$ and $y = +\eta$ shows the left and right positions of the flexible channel boundaries (see

Fig. 3.1). The walls shape can be expressed as

$$y = \pm \eta(x, t) = \pm \left[d_1 + a \sin \frac{2\pi}{\lambda} (x - ct) \right], \quad (3.1)$$

where c is the wave speed, a the wave amplitude, λ the wavelength, $2d_1$ the width of channel and t the time.

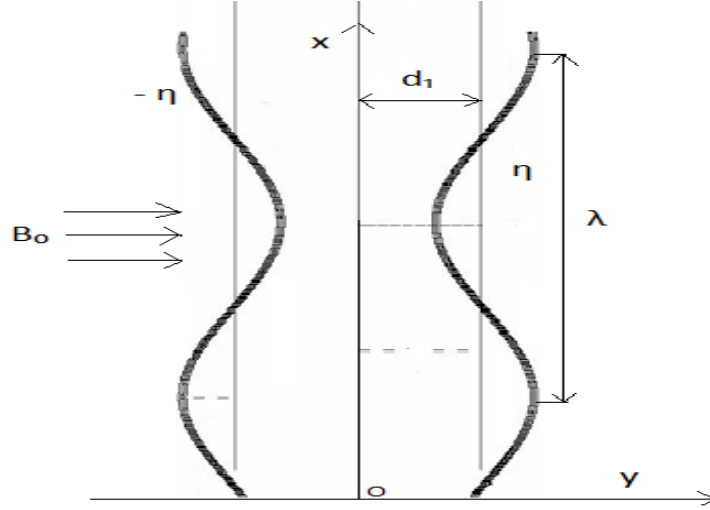


Fig. 3.1. Problem geometry

3.2.1 Magnetohydrodynamics

A magnetic field having strength B_0 is applied with expression as

$$\mathbf{B} = (0, B_0, 0), \quad (3.2)$$

with the negligible induced magnetic field effects. Moreover due to small Reynolds number the electric field is considered absent.

Using Ohm's law the current density \mathbf{J} can be expressed as

$$\mathbf{J} = \sigma [E + \mathbf{V} \times \mathbf{B}], \quad (3.3)$$

Using $\mathbf{V} = (u, v)$ in the above equation we get Lorentz force as

$$\mathbf{J} \times \mathbf{B} = -\sigma B_0^2 u, \quad (3.4)$$

Thus the expression for Joule heating comes out to be

$$\frac{1}{\sigma} \mathbf{J} \cdot \mathbf{J} = \sigma B_0^2 u^2. \quad (3.5)$$

3.2.2 Flow governing equations

Expression of Cauchy stress tensor (τ) for Jeffrey material is

$$\tau = -p\mathbf{I} + \mathbf{S}, \quad (3.6)$$

$$\mathbf{S} = \frac{\mu}{1 + \lambda_1} \left(\dot{\gamma} + \lambda_2 \frac{d\dot{\gamma}}{dt} \right). \quad (3.7)$$

Here \mathbf{S} represent extra stress tensor, λ_1 shows the ratio of relaxation to retardation times, λ_2 the retardation time, p the pressure, \mathbf{I} the identity tensor, μ the absolute viscosity, $\dot{\gamma}$ the shear rate and $\frac{d}{dt}$ the material time differentiation. The equations governing the flow are given by

$$\frac{\partial u}{\partial x} + \frac{\partial v}{\partial y} = 0, \quad (3.8)$$

$$\begin{aligned} \frac{\partial u}{\partial t} + u \frac{\partial u}{\partial x} + v \frac{\partial u}{\partial y} &= -\frac{1}{\rho_f} \frac{\partial p}{\partial x} + \frac{1}{\rho_f} \frac{\partial S_{xx}}{\partial x} + \frac{1}{\rho_f} \frac{\partial S_{xy}}{\partial y} - \frac{\sigma B_0^2 u}{\rho_f} + g\alpha^* (T - T_0) \\ &\quad + g\beta^* (C - C_0), \end{aligned} \quad (3.9)$$

$$\frac{\partial v}{\partial t} + u \frac{\partial v}{\partial x} + v \frac{\partial v}{\partial y} = -\frac{1}{\rho_f} \frac{\partial p}{\partial y} + \frac{1}{\rho_f} \frac{\partial S_{xy}}{\partial x} + \frac{1}{\rho_f} \frac{\partial S_{yy}}{\partial y}, \quad (3.10)$$

$$\begin{aligned} \frac{\partial T}{\partial t} + u \frac{\partial T}{\partial x} + v \frac{\partial T}{\partial y} &= \alpha \left(\frac{\partial^2 T}{\partial x^2} + \frac{\partial^2 T}{\partial y^2} \right) + \frac{1}{\rho_f c_f} \left[S_{xx} \frac{\partial u}{\partial x} + S_{xy} \left(\frac{\partial u}{\partial y} + \frac{\partial v}{\partial x} \right) + S_{yy} \frac{\partial v}{\partial y} \right] \\ &\quad + \tau^* \left[D_B \left(\frac{\partial C}{\partial x} \frac{dT}{dx} + \frac{\partial C}{\partial y} \frac{dT}{dy} \right) + \frac{D_T}{T_m} \left\{ \left(\frac{\partial T}{\partial x} \right)^2 + \left(\frac{\partial T}{\partial y} \right)^2 \right\} \right] \\ &\quad + \frac{1}{\rho_f c_f} \left(\frac{\partial q_r}{\partial y} + \frac{\partial q_r}{\partial x} \right) + \frac{\sigma B_0^2 u^2}{\rho_f c_f}, \end{aligned} \quad (3.11)$$

$$\frac{\partial C}{\partial t} + u \frac{\partial C}{\partial x} + v \frac{\partial C}{\partial y} = D_B \left(\frac{\partial^2 C}{\partial x^2} + \frac{\partial^2 C}{\partial y^2} \right) + \frac{D_T}{T_m} \left(\frac{\partial^2 T}{\partial x^2} + \frac{\partial^2 T}{\partial y^2} \right), \quad (3.12)$$

Radiative heat flux q_r is given by

$$q_r = -\frac{4\sigma^*}{3k^*} \frac{\partial T^4}{\partial y}, \quad (3.13)$$

where σ^* is the Stefan–Boltzmann constant having numerical value $1.380648 \times 10^{-23} JK^{-1}$ and k^* is the mean absorption coefficient. We assume that the temperature difference within the flow is sufficiently small. Hence expanding T^4 about T_0 and neglecting higher order terms one obtains

$$T^4 \cong 4T_0^3 T - 3T_0^4.$$

The above expression and Eq. (3.13) now yield

$$q_r = \frac{-16\sigma^* T_0^3}{3k^*} \frac{\partial T}{\partial y}. \quad (3.14)$$

In vector form q_r can be written as

$$q_r = \frac{-16\sigma^* T_0^3}{3k^*} \nabla T. \quad (3.15)$$

The relevant boundary conditions are

$$u \pm \beta_1 \mu \varepsilon \left(1 + \lambda_2 \left(u \frac{\partial}{\partial x} + v \frac{\partial}{\partial y} \right) \right) \left(\frac{\partial u}{\partial y} + \frac{\partial v}{\partial x} \right) = 0, \quad \text{at } y = \pm \eta, \quad (3.16)$$

$$T \pm \beta_2 \frac{\partial T}{\partial y} = \left(\frac{T_1}{T_0} \right), \quad C \pm \beta_3 \frac{\partial C}{\partial y} = \left(\frac{C_1}{C_0} \right), \quad \text{at } y = \pm \eta, \quad (3.17)$$

$$\begin{aligned} \left[-\tau_1 \frac{\partial^3}{\partial x^3} + m_1 \frac{\partial^3}{\partial x \partial t^2} + d \frac{\partial^2}{\partial x \partial t} \right] \eta &= \frac{\partial S_{xx}}{\partial x} + \frac{\partial S_{xy}}{\partial y} - \rho_f \left(\frac{\partial u}{\partial t} + u \frac{\partial u}{\partial x} + v \frac{\partial u}{\partial y} \right) - \sigma B_0^2 u \\ &\quad - \rho_f g \alpha^* (T - T_0) + \rho_f g \beta^* (C - C_0), \quad \text{at } y = \pm \eta. \end{aligned} \quad (3.18)$$

In the above equations ρ_f describe the nanofluid density, ν the kinematic viscosity, α the thermal diffusivity, σ the thermal conductivity, S_{xx} , S_{xy} , S_{yy} the extra stress tensor components, D_B the Brownian motion coefficient, D_T the thermophoretic diffusion coefficient and $\tau^* = \frac{(\rho c)_p}{(\rho c)_f}$

the ratio of heat capacity of nanomaterial to that of fluid, τ_1 the elastic tension, m_1 the mass per unit area, d the coefficient of viscous damping, $\beta_1, \beta_2, \beta_3$ the slip parameters for velocity, temperature and concentration respectively, T_m the mean temperature, C_1 and T_1 the concentration and temperature at the right wall respectively while C_0 and T_0 the concentration and temperature at the left wall respectively.

3.2.3 Non-dimensional quantities

Various non-dimensional quantities related to the problem are:

$$\begin{aligned} u^* &= \frac{u}{c}, \quad v^* = \frac{v}{c}, \quad x^* = \frac{x}{\lambda}, \quad y^* = \frac{y}{d_1}, \quad \beta_i^* = \frac{\beta_i}{d_1} \quad (i = 1, 2, 3), \quad t^* = \frac{ct}{\lambda}, \quad p^* = \frac{d_1^2 p}{c\lambda\mu}, \\ \eta^* &= \frac{\eta}{d_1}, \quad \theta = \frac{T - T_0}{T_1 - T_0}, \quad \phi = \frac{C - C_0}{C_1 - C_0}, \quad s_{ij} = \frac{d_1}{\mu c} S_{ij}^*, \quad \lambda_2^* = \frac{\lambda_2 c}{d_1}. \end{aligned} \quad (3.19)$$

3.2.4 Utilization of stream function

Eqs.(3.9)–(3.12) after omitting asterisks and writing stream function $\psi(x, y, t)$ by the definition [7]:

$$u = \frac{\partial \psi}{\partial y}, \quad v = -\delta \frac{\partial \psi}{\partial x},$$

become

$$\begin{aligned} \text{Re} \left[\delta \frac{\partial^2 \psi}{\partial t \partial y} + \delta \frac{\partial \psi}{\partial y} \frac{\partial^2 \psi}{\partial x \partial y} - \delta \frac{\partial \psi}{\partial x} \frac{\partial^2 \psi}{\partial y^2} \right] &= -\frac{\partial p}{\partial x} + \delta \frac{\partial s_{xx}}{\partial x} + \frac{\partial s_{xy}}{\partial y} \\ &\quad + Gr\theta + Qr\phi - M^2 u, \end{aligned} \quad (3.20)$$

$$\text{Re} \delta \left[-\delta^2 \frac{\partial^2 \psi}{\partial x \partial t} - \delta^2 \frac{\partial \psi}{\partial y} \frac{\partial^2 \psi}{\partial x^2} - \delta^2 \frac{\partial^2 \psi}{\partial x \partial y} \right] = -\frac{\partial p}{\partial y} + \delta^2 \frac{\partial s_{xy}}{\partial x} + \delta \frac{\partial s_{yy}}{\partial y}, \quad (3.21)$$

$$\begin{aligned}
\text{Re} \left[\delta \frac{\partial \theta}{\partial t} + u \delta \frac{\partial \theta}{\partial x} + v \frac{\partial \theta}{\partial y} \right] &= Ec \left(\frac{1}{1 + \lambda_1} \right) \left[\left(1 + \lambda_2^* \delta \left(\frac{\partial \psi}{\partial y} \frac{\partial}{\partial x} - \frac{\partial \psi}{\partial x} \frac{\partial}{\partial y} \right) \right) \right. \\
&\quad \left. \left(4\delta^2 \left(\frac{\partial^2 \psi}{\partial x \partial y} \right)^2 + \left(-\delta^2 \frac{\partial^2 \psi}{\partial x^2} + \frac{\partial^2 \psi}{\partial y^2} \right)^2 \right) \right] \\
&\quad + Rn \left(\delta \frac{\partial^2 \theta}{\partial x \partial y} + \frac{\partial^2 \theta}{\partial y^2} \right) + \frac{1}{\text{Pr}} \left(\delta^2 \frac{\partial^2 \theta}{\partial x^2} + \frac{\partial^2 \theta}{\partial y^2} \right) + Ec M^2 \left(\frac{\partial \psi}{\partial y} \right)^2 \\
&\quad + Nb \left[\delta^2 \frac{\partial \phi}{\partial x} \frac{\partial \theta}{\partial x} + \frac{\partial \phi}{\partial y} \frac{\partial \theta}{\partial y} \right] + Nt \left[\left(\delta \frac{\partial \theta}{\partial x} \right)^2 + \left(\frac{\partial \theta}{\partial y} \right)^2 \right], \quad (3.22)
\end{aligned}$$

$$\text{Re} Sc \left[\delta \frac{\partial \phi}{\partial t} + \delta \frac{\partial \psi}{\partial y} \frac{\partial \phi}{\partial x} - \delta \frac{\partial \psi}{\partial x} \frac{\partial \phi}{\partial y} \right] = \left(\delta^2 \frac{\partial^2 \phi}{\partial x^2} + \frac{\partial^2 \phi}{\partial y^2} \right) + \frac{Nt}{Nb} \left(\delta^2 \frac{\partial^2 \theta}{\partial x^2} + \frac{\partial^2 \theta}{\partial y^2} \right), \quad (3.23)$$

with the boundary conditions

$$\frac{\partial \psi}{\partial y} \pm \beta_1 \varepsilon \left[1 + \lambda_2^* \delta \left(\frac{\partial \psi}{\partial y} \frac{\partial}{\partial x} - \delta^2 \frac{\partial \psi}{\partial x} \frac{\partial}{\partial y} \right) \right] \left(\frac{\partial^2 \psi}{\partial y^2} - \delta \frac{\partial^2 \psi}{\partial x^2} \right) = 0, \quad \text{at } y = \pm \eta, \quad (3.24)$$

$$\theta \pm \beta_2 \frac{\partial \theta}{\partial y} = \begin{pmatrix} 1 \\ 0 \end{pmatrix}, \quad \phi \pm \beta_3 \frac{\partial \phi}{\partial y} = \begin{pmatrix} 1 \\ 0 \end{pmatrix}, \quad \text{at } y = \pm \eta, \quad (3.25)$$

$$\begin{aligned}
\left[E_1 \frac{\partial^3}{\partial x^3} + E_2 \frac{\partial^3}{\partial x \partial t^2} + E_3 \frac{\partial^2}{\partial x \partial t} \right] \eta &= \varepsilon \left(1 + \delta \frac{\partial \psi}{\partial y} \frac{\partial}{\partial x} \right) \frac{\partial^3 \psi}{\partial y^3} \\
&+ Gr \theta + Qr \phi - M^2 \frac{\partial \psi}{\partial y}, \quad \text{at } y = \pm \eta, \quad (3.26)
\end{aligned}$$

where

$$\begin{aligned}
s_{xx} &= 2\delta \varepsilon \left[1 + \lambda_2^* \delta \left(\frac{\partial \psi}{\partial y} \frac{\partial}{\partial x} - \frac{\partial \psi}{\partial x} \frac{\partial}{\partial y} \right) \right] \frac{\partial^2 \psi}{\partial x \partial y}, \\
s_{xy} &= \varepsilon \left[1 + \lambda_2^* \delta \left(\frac{\partial \psi}{\partial y} \frac{\partial}{\partial x} - \frac{\partial \psi}{\partial x} \frac{\partial}{\partial y} \right) \right] \left(\frac{\partial^2 \psi}{\partial y^2} - \delta^2 \frac{\partial^2 \psi}{\partial x^2} \right), \\
s_{yy} &= -2\delta \varepsilon \left[1 + \lambda_2^* \delta \left(\frac{\partial \psi}{\partial y} \frac{\partial}{\partial x} - \frac{\partial \psi}{\partial x} \frac{\partial}{\partial y} \right) \right] \frac{\partial^2 \psi}{\partial x \partial y},
\end{aligned}$$

Implication of long wavelength and low Reynolds number approximations [18] reduce the problem as follows:

$$\varepsilon \frac{\partial^4 \psi}{\partial y^4} + Gr \frac{\partial \theta}{\partial y} + Qr \frac{\partial \phi}{\partial y} - M^2 \frac{\partial^2 \psi}{\partial y^2} = 0, \quad (3.27)$$

$$(1 + Rn \text{Pr}) \frac{\partial^2 \theta}{\partial y^2} + Nb \text{Pr} \frac{\partial \theta}{\partial y} \frac{\partial \phi}{\partial y} + Nt \text{Pr} \left(\frac{\partial \theta}{\partial y} \right)^2 + Br \left[\frac{1}{1 + \lambda_1} \left(\frac{\partial^2 \psi}{\partial y^2} \right)^2 + M^2 \left(\frac{\partial \psi}{\partial y} \right)^2 \right] = 0, \quad (3.28)$$

$$\frac{\partial^2 \phi}{\partial y^2} + \frac{Nt}{Nb} \left(\frac{\partial^2 \theta}{\partial y^2} \right) = 0, \quad (3.29)$$

$$\frac{\partial \psi}{\partial y} \pm \beta_1 \varepsilon \left(\frac{\partial^2 \psi}{\partial y^2} \right) = 0, \theta \pm \beta_2 \frac{\partial \theta}{\partial y} = \begin{pmatrix} 1 \\ 0 \end{pmatrix}, \phi \pm \beta_3 \frac{\partial \phi}{\partial y} = \begin{pmatrix} 1 \\ 0 \end{pmatrix}, \quad \text{at } y = \pm \eta, \quad (3.30)$$

$$\left[E_1 \frac{\partial^3}{\partial x^3} + E_2 \frac{\partial^3}{\partial x \partial t^2} + E_3 \frac{\partial^2}{\partial x \partial t} \right] \eta = \varepsilon \frac{\partial^3 \psi}{\partial y^3} + Gr \theta + Qr \phi - M^2 \frac{\partial \psi}{\partial y}, \quad \text{at } y = \pm \eta, \quad (3.31)$$

where $\varepsilon = \frac{1}{1 + \lambda_1}$, $\epsilon = \frac{a}{d_1}$ represents the amplitude ratio, $\delta = \frac{d_1}{\lambda}$ the wave number, $Nb = \frac{\tau^* D_B (C_1 - C_0)}{\nu}$ the Brownian motion parameter, $Nt = \frac{\tau^* D_T (T_1 - T_0)}{T_m \nu}$ the thermophoresis parameter, $Re = \frac{c \rho_f d_1}{\mu}$ the Reynolds number, $Sc = \frac{\nu}{D_B}$ the Schmidt number, $M = \sqrt{\frac{\sigma}{\mu}} B_0 d_1$ the Hartman number, $Ec = \frac{c^2}{C_p (T_1 - T_0)}$ the Eckert number, $Pr = \frac{\nu \rho c_p}{k}$ the Prandtl number, $Gr = \frac{g \alpha^* (T_1 - T_0) d_1^2}{\nu c}$ the Grashoff number, $Qr = \frac{g \beta^* (C_1 - C_0) d_1^2}{\nu c}$ the Grashoff number for nanoparticles, $Rn = \frac{16 \sigma^* T_0^3}{3 k^* \mu C_p}$ the radiation parameter, $Br = Pr Ec$ the Brinkman number, Ec the Eckert number, $E_1 = -\frac{\tau_1 d_1^3}{\lambda^3 \mu c}$, $E_2 = \frac{m_1 d_1^3 c}{\lambda^3 \mu}$ and $E_3 = \frac{d d_1^3}{\lambda^2 \mu}$ the wall parameters.

3.3 Discussion

The aim of this section is to predict the behavior of velocity, temperature, heat transfer and concentration of nanoparticles in response to relevant parameters. Thus plots obtained through built-in command *NDSolve* of Mathematica together with their physical explanations are presented here.

3.3.1 Velocity profile

This portion represents impact of emerging parameters on velocity. In (Fig. 3.2) it is observed that for larger velocity slip parameter β_1 , the velocity increases. As fluid slip is the deviation in the angle at which the fluid leaves the channel. Therefore an increase in β_1 causes non-uniform velocity distribution inside the channel (see Fig. 3.2). The effect is useful in determining the accurate estimation of energy transfer between the channel and the fluid. Similar result has been

obtained by Hayat et. al [13] in their study for nanofluids. The reason behind the increasing behavior of β_1 is that the resistance is reduced due to slip hence velocity increases. Reduction in drag forces corresponding to Grashoff number Gr increases the velocity (see Fig. 3.3). It is seen that velocity enhances for both Jeffrey fluid parameter λ_1 and mass transfer Grashoff number Qr (see Figs. 3.4 and 3.5). The decelerating character of magnetic field compresses the fluid particles and thus reducing velocity profile for greater values of Hartman number M (see Fig. 3.6). The elastic wall properties E_1 and E_2 causes enhancement in velocity while damping effect E_3 decreases it (see Fig. 3.7). For reliability the results obtained for wall parameters can be compared with the previous analysis of Hina et al. [11] for curved channel and Hayat et al. [13] for planer channel.

3.3.2 Temperature profile

Physical illustration of the temperature is displayed in this part of the chapter. For larger thermal slip parameter β_2 temperature increases as seen from Fig. 3.8. Fig. 3.9 is plotted to see the behavior of temperature profile for different values of Brinkman number Br . Here viscous dissipation causes enhancement in temperature. It is reasonable to say that rise in temperature is produced by the stress-reversal process that develops with an increase in Br (see Fig. 3.9). The similar observation for Carreau fluid have been reported by Vajravelu et al. [15]. Larger values of Jeffrey nanofluid parameter λ_1 enhances the temperature (see Fig. 3.10). Motion of fluid particles is slowed down due to decreased kinetic energy thus temperature decreases on application of magnetic force. Thus Hartman number M decays the temperature (see Fig. 3.11). Here the obtained numerical results are found well matched with the perturbed results by Hayat et al. [7]. Temperature is more for increasing values of Brownian motion parameter Nb (see Fig. 3.12). However for thermophoresis parameter Nt it decreases (see Fig. 3.13). Since nanoparticles possess strong thermal gradients producing nonlinear dependence of the drift velocity on the applied gradient for large Nt . Thus nonlinear thermophoresis can cause contradictory results between thermophoretic and numerical analysis. That is why the numerical results develops the nonlinear temperature distribution with Nt similar to the study of Hayat et al. [13]. Temperature rises for larger Prandtl number Pr (see Fig. 3.14). It is in view of an increase in specific heat. An increase in thermal radiation parameter Rn decreases

the temperature (as noticed from Fig. 3.15). Temperature is the increasing functions of E_1 and E_2 due to elastance of wall while it decreases for E_3 as E_3 shows oscillatory resistance (see Fig. 3.16).

3.3.3 Nanoparticle concentration profile

Various illustrations for concentration profile are presented here. It is noticed that by increasing values of concentration slip parameter β_3 the nanoparticle concentration decreases (see Fig. 3.17). Fig. 3.18 portrays a decay in concentration for Jeffrey nanofluid parameter λ_1 . Nanoparticle concentration is more for Brownian motion (as seen from Fig. 3.19) and less for thermophoresis (as noticed from Fig. 3.20). Fig. 3.21 depicts that concentration reduces for E_1 and E_2 while it enhances for E_3 .

3.3.4 Heat transfer coefficient

The non-dimensional form of heat transfer coefficient is

$$Z = \eta_x \frac{\partial \theta}{\partial y} \Big|_{y=\pm\eta} . \quad (3.32)$$

The motion of peristaltic walls is considered responsible for the oscillatory behavior of heat transfer coefficient. For thermal slip parameter β_2 the absolute value of Z decreases (see Fig. 3.22). Increasing heat transfer rate is noticed for Prandtl number Pr (see Fig. 3.23). Also larger radiation parameter Rn enhances the heat transfer coefficient Z (see Fig. 3.24).

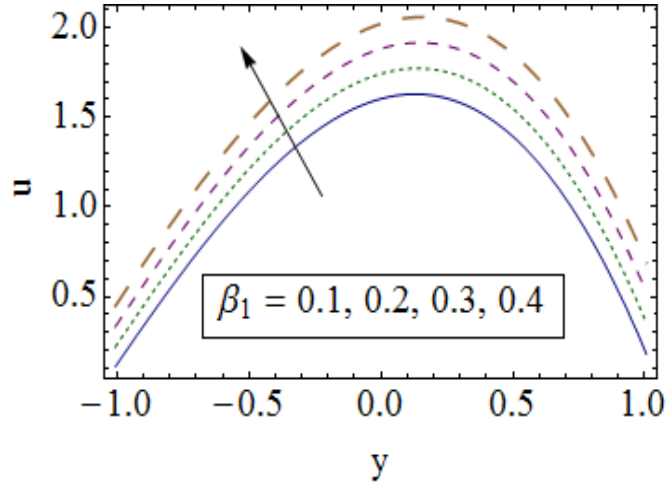


Fig. 3.2.

Fig. 3.2. Sketch of u for β_1 when $x = 0.2$, $t = 0.1$, $Pr = 1.5$, $Nt = Nb = 0.1$, $Br = 1.7$, $Qr = 1$, $Gr = 1.5$, $\epsilon = 0.2$, $M = 0.2$, $E_1 = E_3 = 0.01$, $E_2 = 0.02$, $\beta_2 = 0.1$, $\beta_3 = 0.1$, $\lambda_1 = 1$, $Rn = 1$.

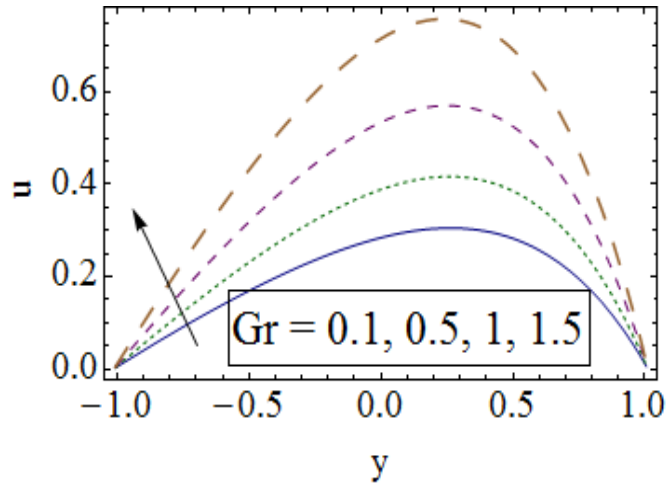


Fig. 3.3.

Fig. 3.3. Sketch of u for Gr when $x = 0.2$, $t = 0.1$, $Pr = 0.8$, $Nt = 0.3$, $Nb = 0.2$, $Br = 1.7$, $Qr = 1$, $\epsilon = 0.2$, $M = 1$, $E_1 = 0.01$, $E_2 = 0.02$, $E_3 = 0.01$, $\beta_1 = 0.1$, $\beta_2 = 0.1$, $\beta_3 = 0.1$, $\lambda_1 = 1$, $Rn = 1$.

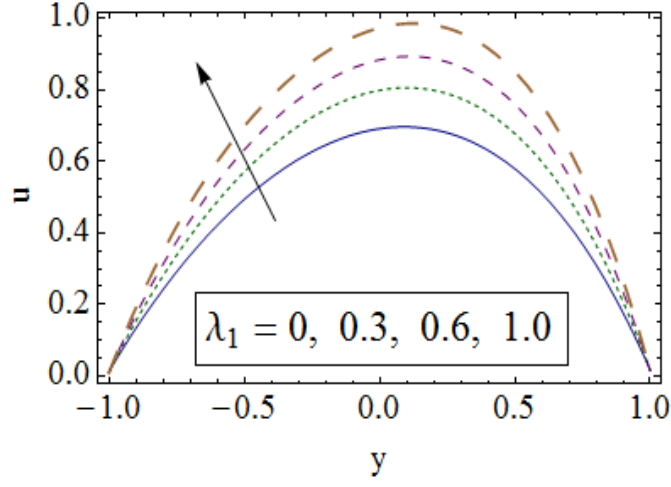


Fig. 3.4.

Fig. 3.4. Sketch of u for λ_1 when $x = 0.2$, $t = 0.1$, $Pr = 0.8$, $Nt = 0.3$, $Nb = 0.2$, $Nt = 1.7$, $Qr = 1$, $Gr = 0.5$, $\epsilon = 0.2$, $M = 1$, $E_1 = 0.01$, $E_2 = 0.02$, $E_3 = 0.01$, $\beta_1 = 0.1$, $\beta_2 = 0.1$, $\beta_3 = 0.1$, $Rn = 1$.

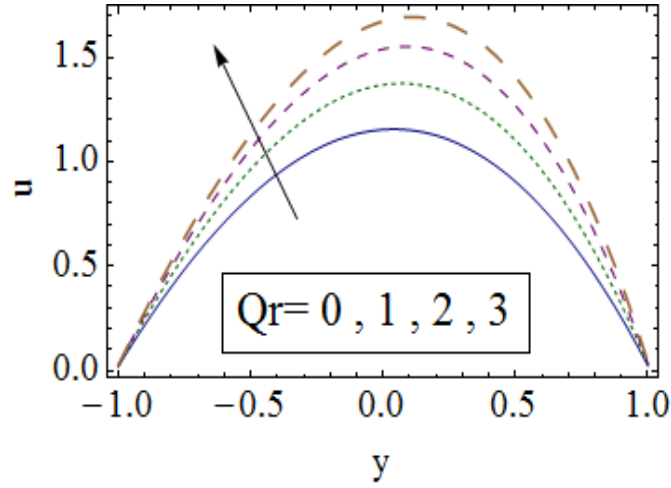


Fig. 3.5.

Fig. 3.5. Sketch of u for Qr when $x = 0.2$, $t = 0.1$, $Pr = 1$, $Nt = 0.1$, $Nb = 0.1$, $Br = 1.7$, $Gr = 1.5$, $\epsilon = 0.2$, $M = 0.2$, $E_1 = 0.01$, $E_2 = 0.02$, $E_3 = 0.01$, $\beta_1 = 0.1$, $\beta_2 = 0.1$, $\beta_3 = 0.1$, $\lambda_1 = 0.1$, $Rn = 1$.

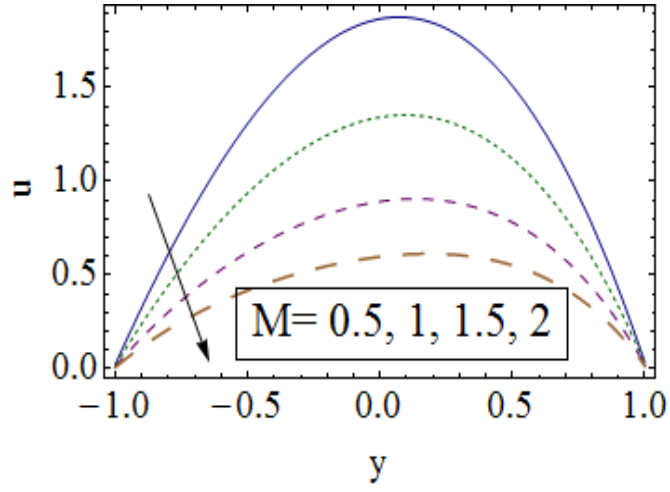


Fig. 3.6.

Fig. 3.6. Sketch of u for M when $x = 0.2$, $t = 0.1$, $Pr = 1$, $Nt = 0.1$, $Nb = 0.1$, $Br = 0.5$, $Qr = 0.3$, $Gr = 1$, $\epsilon = 0.2$, $E_1 = E_3 = 0.01$, $E_2 = 0.02$, $\beta_1 = 0.1$, $\beta_2 = 0.1$, $\beta_3 = 0.1$, $\lambda_1 = 1$, $Rn = 1$.

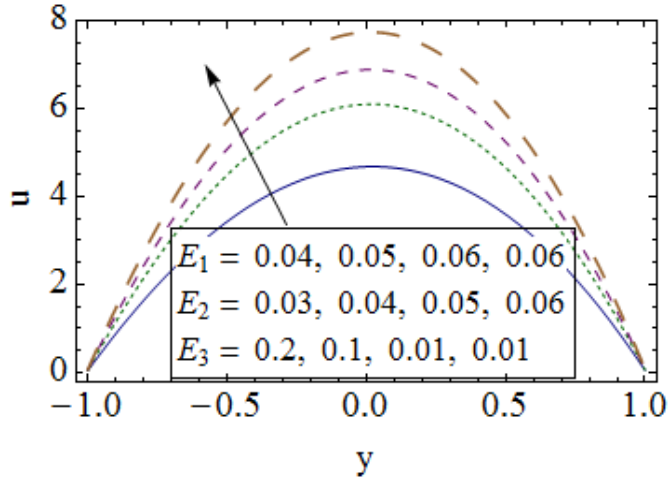


Fig. 3.7.

Fig. 3.7. Sketch of u for E_1, E_2, E_3 when $x = 0.2$, $t = 0.1$, $Pr = 1.5$, $Nt = 0.1$, $Nb = 0.1$, $Br = 1.7$, $Qr = 1$, $Gr = 1.5$, $\epsilon = 0.2$, $M = 0.2$, $\beta_1 = 0.1$, $\beta_2 = 0.1$, $\beta_3 = 0.1$, $\lambda_1 = 1$, $Rn = 1$.

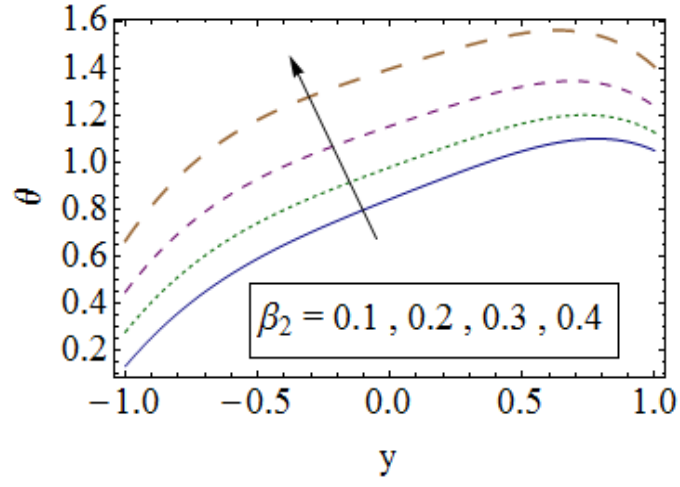


Fig. 3.8.

Fig. 3.8. Sketch of θ for β_2 when $x = \epsilon = 0.2$, $t = 0.1$, $Rn = 1$, $Gr = 1$, $Qr = 0.3$, $\lambda_1 = 1$, $Br = 0.5$, $Pr = 1$, $Nt = Nb = 0.1$, $M = 0.2$, $\beta_1 = \beta_3 = 0.1$, $E_1 = E_3 = 0.01$, $E_2 = 0.02$.

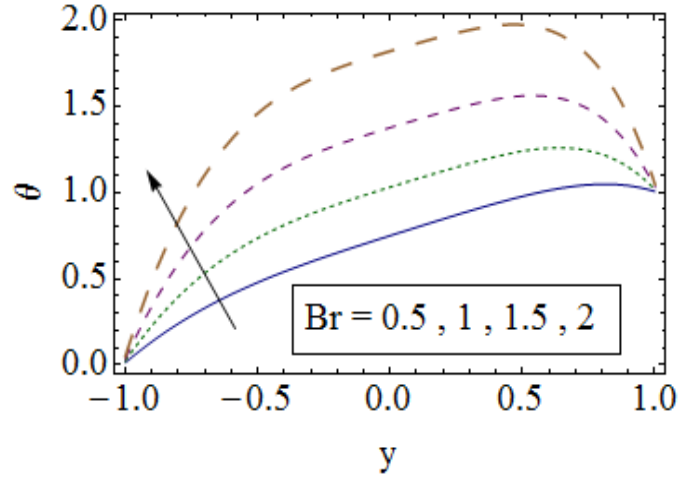


Fig. 3.9.

Fig. 3.9. Sketch of θ for Br when $x = \epsilon = 0.2$, $t = 0.1$, $\lambda_1 = 0.3$, $Rn = 1$, $Gr = 1.5$, $Qr = 1$, $Pr = 1$, $Nt = Nb = 0.1$, $M = 0.2$, $\beta_1 = \beta_2 = \beta_3 = 0.1$, $E_1 = E_3 = 0.01$, $E_2 = 0.02$.

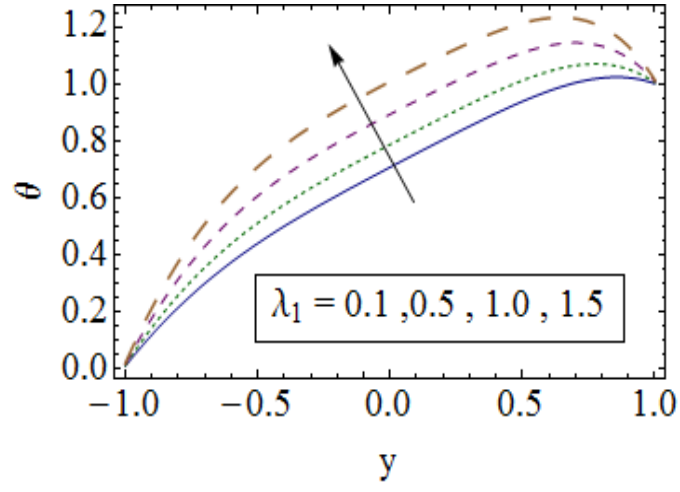


Fig. 3.10.

Fig. 3.10. Sketch of θ for λ_1 when $x = \epsilon = 0.2$, $t = 0.1$, $Rn = 1$, $Gr = 1.5$, $Qr = 1$, $Br = 0.5$, $Pr = 1$, $Nt = Nb = 0.1$, $M = 0.2$, $\beta_1 = \beta_2 = \beta_3 = 0.1$, $E_1 = E_3 = 0.01$, $E_2 = 0.02$.

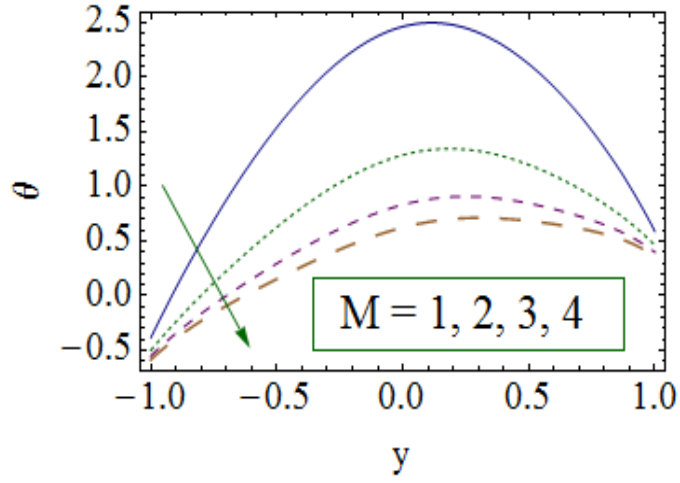


Fig. 3.11.

Fig. 3.11. Sketch of θ for M when $x = \epsilon = 0.2$, $t = 0.1$, $Qr = 1$, $Rn = 1$, $Gr = 1.5$, $Qr = 1$, $\lambda_1 = 0.3$, $Br = 0.5$, $Pr = 1$, $Nt = Nb = 0.1$, $\beta_1 = \beta_2 = \beta_3 = 0.1$, $E_1 = E_3 = 0.01$, $E_2 = 0.02$.

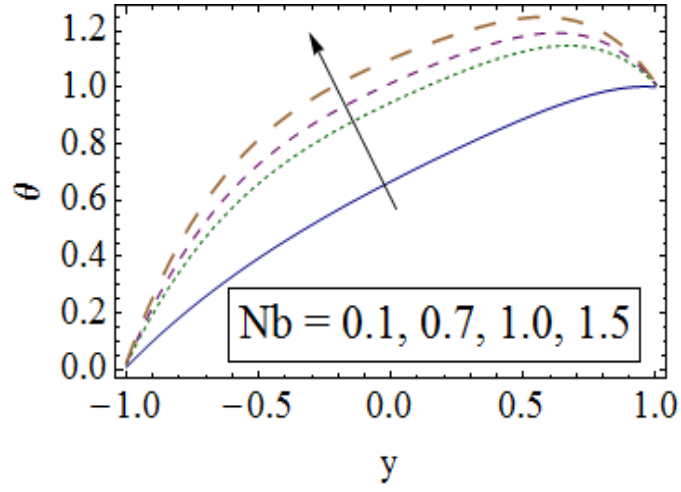


Fig. 3.12.

Fig. 3.12. Sketch of θ for Nb when $x = \epsilon = 0.2$, $t = 0.1$, $Rn = 1$, $Gr = 1.5$, $Qr = 0.3$, $\lambda_1 = 1$, $Br = 0.5$, $Pr = 1$, $Nt = 0.1$, $M = 0.5$, $\beta_1 = \beta_2 = \beta_3 = 0.1$, $E_1 = E_3 = 0.01$, $E_2 = 0.02$.

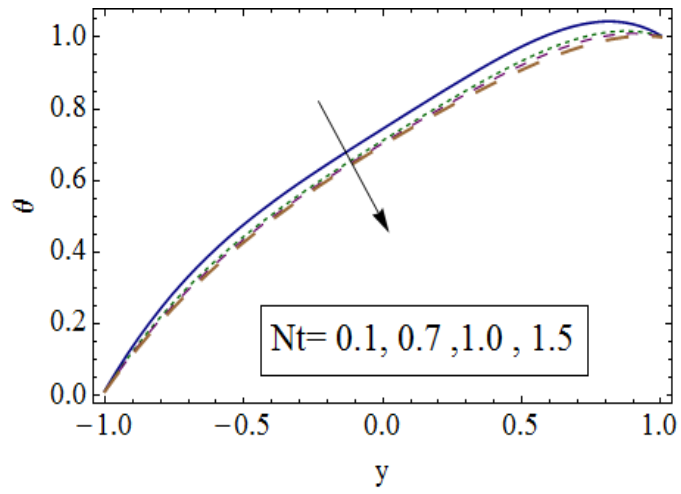


Fig. 3.13.

Fig. 3.13. Sketch of θ for Nt when $x = \epsilon = 0.2$, $t = 0.1$, $Rn = 1$, $Gr = 1$, $Qr = 0.3$, $\lambda_1 = 1$, $Br = 0.5$, $Pr = 1$, $Nb = 0.1$, $M = 0.2$, $\beta_1 = \beta_2 = \beta_3 = 0.1$, $E_1 = E_3 = 0.01$, $E_2 = 0.02$.

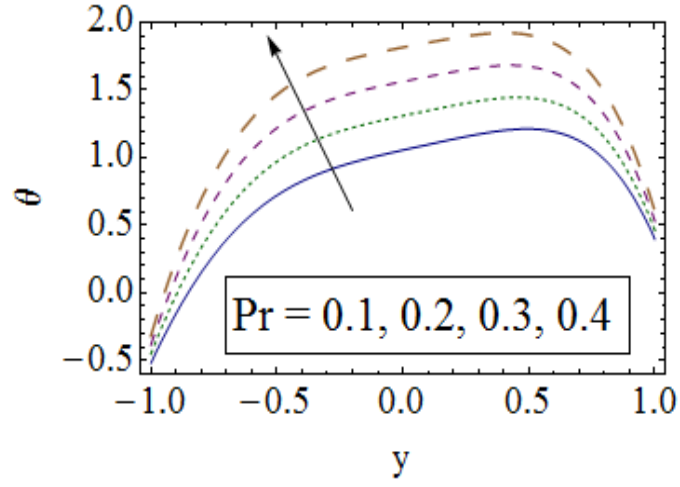


Fig. 3.14.

Fig. 3.14. Sketch of θ for Pr when $x = \epsilon = 0.2$, $t = 0.1$, $Rn = 2$, $Gr = 1.5$, $Qr = 0.3$, $\lambda_1 = 1$, $Br = 1.7$, $Nt = 0.1$, $Nb = 1$, $M = 0.2$, $\beta_1 = \beta_2 = \beta_3 = 0.1$, $E_1 = E_3 = 0.01$, $E_2 = 0.02$.

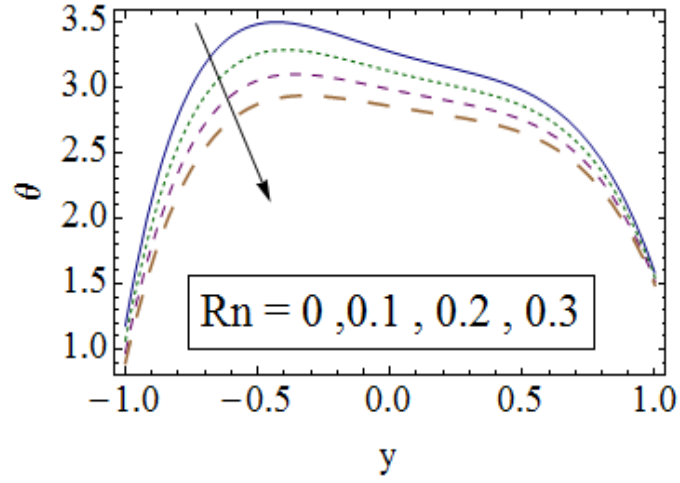


Fig. 3.15.

Fig. 3.15. Sketch of θ for Rn when $x = \epsilon = 0.2$, $t = 0.1$, $Gr = 1.5$, $Qr = 0.3$, $\lambda_1 = 1$, $Br = 1.7$, $Pr = 1$, $Nt = 3$, $Nb = 2$, $M = 0.2$, $\beta_1 = \beta_2 = \beta_3 = 0.1$, $E_1 = E_3 = 0.01$, $E_2 = 0.02$.

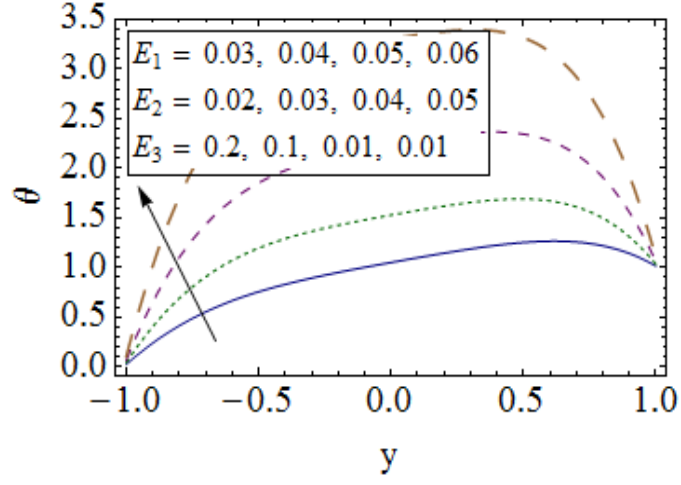


Fig. 3.16.

Fig. 3.16. Sketch of θ for E_1, E_2, E_3 when $x = \epsilon = 0.2, t = 0.1, Gr = 1, Qr = 1, Rn = 1, Gr = 1, Qr = 0.3, \lambda_1 = 1, Br = 0.5, Pr = 1, Nt = Nb = 0.1, M = 0.2, \beta_1 = \beta_2 = \beta_3 = 0.1$.

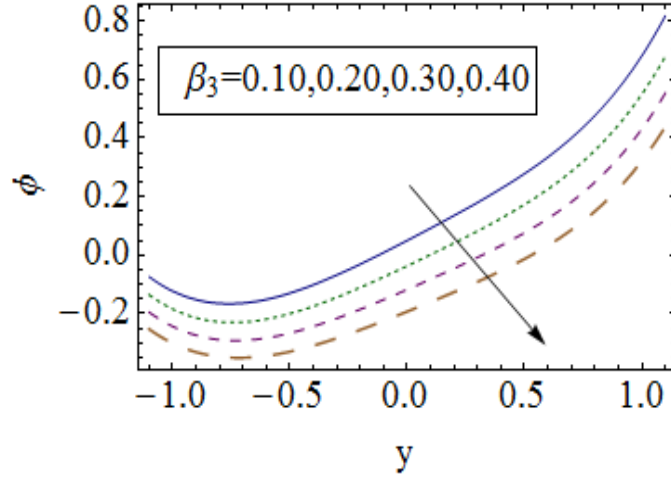


Fig. 3.17.

Fig. 3.17. Sketch of ϕ for β_3 when $x = \epsilon = 0.2, t = 0.1, Gr = 1, Qr = 0.3, Br = 0.5, Nt = Nb = 0.1, Pr = 1, M = 0.2, \lambda_1 = 1, Rn = 1, \beta_1 = \beta_2 = 0.1, E_1 = E_3 = 0.01, E_2 = 0.02$.

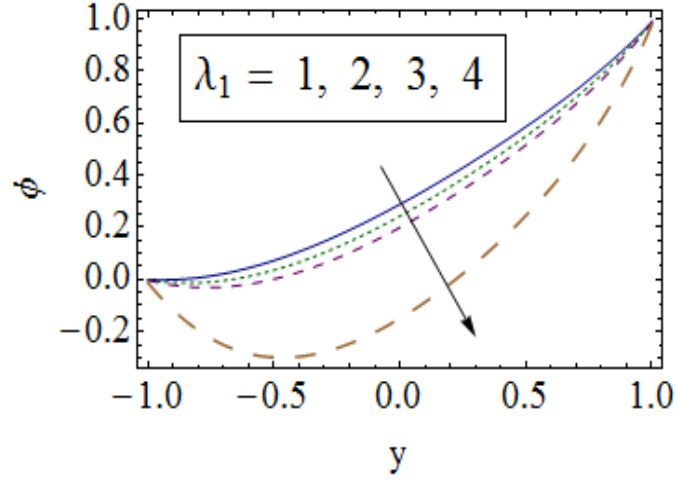


Fig. 3.18.

Fig. 3.18. Sketch of ϕ for λ_1 when $x = \epsilon = 0.2$, $t = 0.1$, $Gr = 0.8$, $Qr = 1$, $Pr = 1$, $Br = 1.7$, $M = 0.2$, $Rn = 1$, $\beta_1 = \beta_2 = \beta_3 = 0.1$, $E_1 = E_3 = 0.01$, $E_2 = 0.02$.

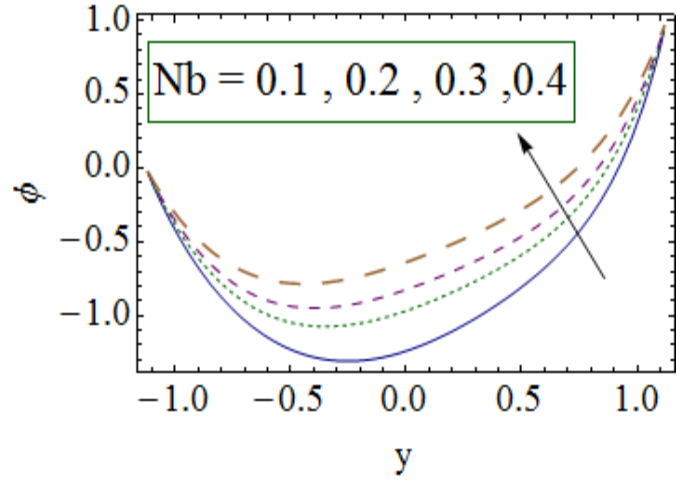


Fig. 3.19.

Fig. 3.19. Sketch of ϕ for Nb when $x = \epsilon = 0.2$, $t = 0.1$, $Gr = 0.8$, $Qr = 0.3$, $Br = 1.7$, $Nt = 0.1$, $Pr = 1$, $M = 0.2$, $\lambda_1 = 1$, $Rn = 1$, $\beta_1 = \beta_2 = \beta_3 = 0.1$, $E_1 = E_3 = 0.01$, $E_2 = 0.02$.

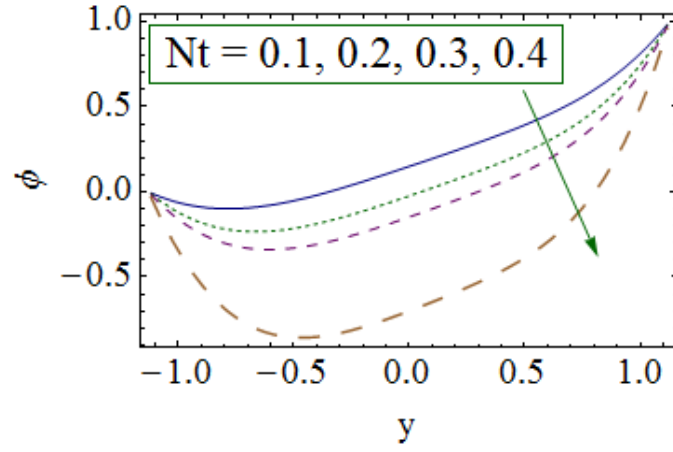


Fig. 3.20.

Fig. 3.20. Sketch of ϕ for Nt when $x = \epsilon = 0.2$, $t = 0.1$, $Gr = 1$, $Br = 1.7$, $Qr = 0.3$, $\lambda_1 = 1$, $Rn = 1$, $Nb = 0.3$, $Pr = 1$, $M = 0.2$, $\beta_1 = \beta_2 = \beta_3 = 0.1$, $E_1 = E_3 = 0.01$, $E_2 = 0.02$.

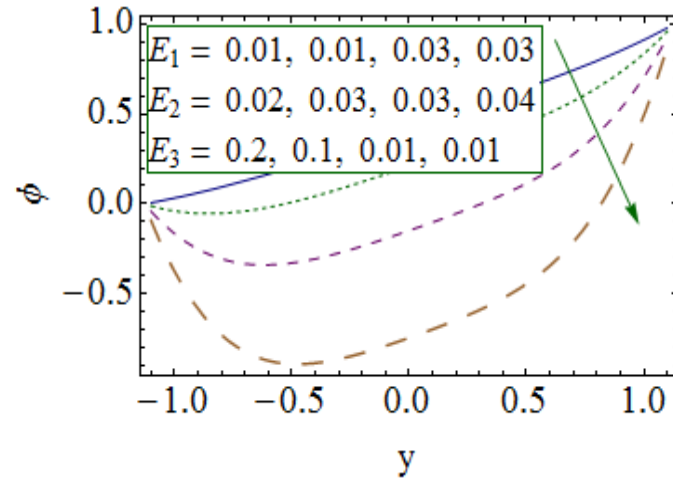


Fig. 3.21.

Fig. 3.21. Sketch of ϕ for E_1, E_2, E_3 when $x = \epsilon = 0.2$, $t = 0.1$, $\beta_1 = \beta_2 = \beta_3 = 0.1$, $Gr = 1$, $Qr = 0.3$, $Br = 0.5$, $Nt = Nb = 0.1$, $Pr = 1$, $M = 0.2$, $\lambda_1 = 1$, $Rn = 1$, $\beta_1 = \beta_2 = \beta_3 = 0.1$.

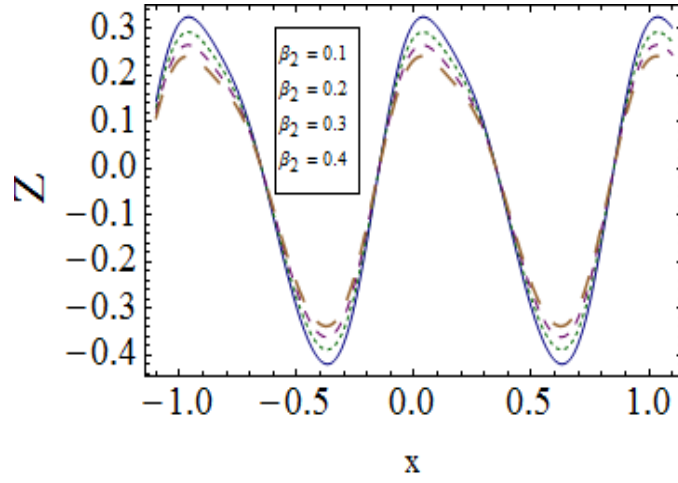


Fig. 3.22.

Fig. 3.22. Sketch of Z for β_2 when $\epsilon = 0.2$, $t = 0.1$, $Rn = 2$, $Gr = 0.3$, $Qr = 1$, $\lambda_1 = 1$, $Br = 0.5$, $Pr = 1$, $Nt = Nb = 1$, $M = 2$, $\beta_1 = \beta_3 = 0.1$, $E_1 = 0.1$, $E_3 = 0.01$, $E_2 = 0.2$.

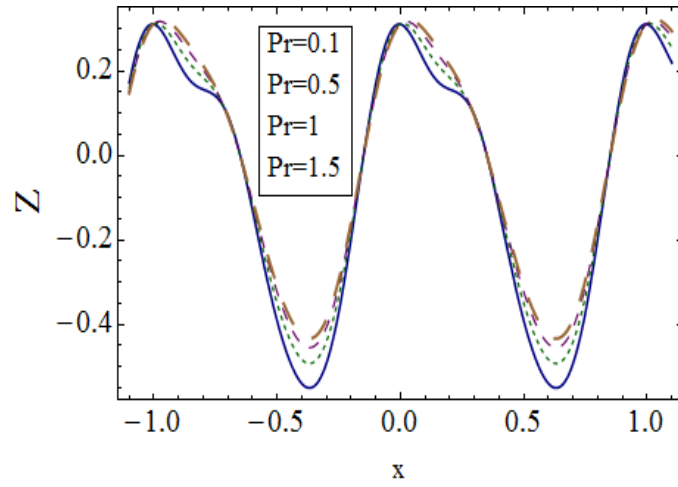


Fig. 3.23.

Fig. 3.23. Sketch of Z for Pr when $\epsilon = 0.2$, $t = 0.1$, $\lambda_1 = 1$, $Rn = 2$, $Gr = 0.3$, $Qr = 1$, $Nt = Nb = 1$, $M = 2$, $\beta_1 = \beta_2 = \beta_3 = 0.1$, $Br = 1.8$, $E_1 = 0.1$, $E_3 = 0.01$, $E_2 = 0.2$.

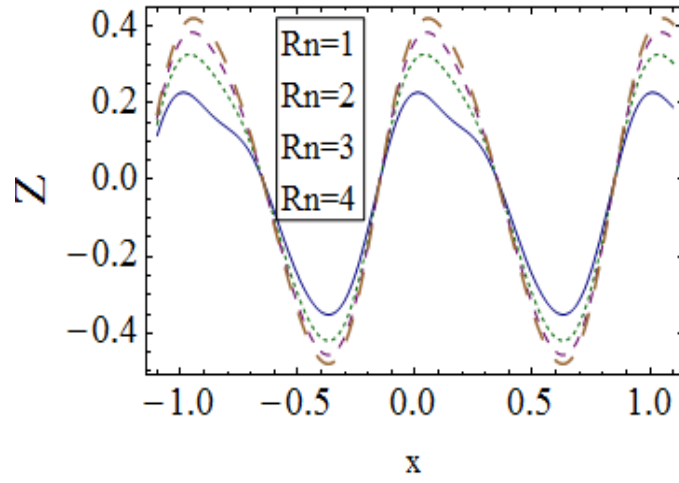


Fig. 3.24.

Fig. 3.24. Sketch of Z for Rn when $\epsilon = 0.2$, $t = 0.1$, $Gr = 0.3$, $Qr = 1$, $Br = 0.4$, $Nt = Nb = 0.1$, $M = 2$, $Pr = 0.8$, $\beta_1 = \beta_2 = \beta_3 = 0.1$, $E_1 = 0.1$, $E_3 = 0.01$, $E_2 = 0.2$.

3.4 Conclusion

Peristaltic flow of Jeffrey nanofluid in a channel having compliant walls is addressed here. The effects of partial slip and mixed convection are present. The major observations are listed below:

- Behavior of λ_1 on velocity and temperature is similar.
- Concentration and temperature have reverse effect for λ_1 .
- An enhancement in the velocity is observed for heat and mass transfer Grashoff numbers Gr and Qr .
- Qualitatively same effects on temperature is obtained for radiation Rn and thermophoresis parameter Nt .
- Effects of E_1 and E_2 on velocity are similar. Whereas the impact of E_3 on velocity is opposite to that of E_1 and E_2 .
- Behaviors of β_1 on velocity and β_2 on temperature are similar. However concentration decreases upon increasing slip parameter β_3 .
- Hartman number M reduces the temperature and velocity.
- Both temperature and heat transfer coefficient are increased for Prandtl number Pr .
- Concentration is decreasing function of E_1 and E_2 . However the role of E_3 on concentration is reverse to that of E_1 and E_2 .

Bibliography

- [1] T. W. Latham, Fluid motion in peristaltic pumps, MS. Thesis, MIT, Cambridge, MA, 1966.
- [2] A. H. Shapiro, M. Y. Jaffrin and S. L. Weinberg, Peristaltic pumping with long wavelengths at low Reynolds number, *J. Fluid Mech.*, 37 (1969) 799 – 825.
- [3] T. Hayat, H. Yasmin and M. Al-Yami, Soret and Dufour effects in peristaltic transport of physiological fluids with chemical reaction, A mathematical analysis, *Comp. Fluids*, 89 (2014) 242 – 253.
- [4] Kh. S. Mekheimer, Y. Abd elmabond and A. I. Abdellateef, Peristaltic transport through eccentric cylinders, Mathematical model, *Appl. Bio. Biomech.*, 10 (2013) 19 – 27.
- [5] D. Tripathi and O. A. Beg, A study on peristaltic flow of nanofluids: Application in drug delivery systems, *Int. J. Heat Mass Transf.*, 70 (2014) 61 – 70.
- [6] T. Hayat, F. M. Abbasi, A. Alsaedi, and F. Alsaadi, Hall and Ohmic Heating Effects on the Peristaltic transport of a Carreau–Yasuda fluid in an asymmetric channel, *ZNA*, 69 (2014) 43 – 51.
- [7] T. Hayat, A. Tanveer, H. Yasmin and A. Alsaedi, Homogeneous-Heterogeneous Reactions in Peristaltic flow with convective conditions, *PLOS ONE*, 9 (2014) e113851.
- [8] F. M. Abbasi, T. Hayat and B. Ahmad, Peristaltic transport of copper–water nanofluid saturating porous medium, *Physica E*., 67 (2015) 47 – 53.

- [9] T. Hayat, F. M. Abbasi and F. Alsaedi, Hydromagnetic peristaltic transport of water-based nanofluids with slip effects through an asymmetric channel, *Int. J. Mode. Phy.*, 29 (2015) (17 pages).
- [10] R. Ellahi, M. M. Bhatti and K. Vafai, Effects of heat and mass transfer on peristaltic flow in a non-uniform rectangular duct, *Int. J. Heat Mass Transf.*, 71 (2014) 706 – 719.
- [11] S. Hina, T. Hayat, M. Mustafa and A. Alsaedi, Peristaltic transport of pseudoplastic fluid in a curved channel with wall properties and slip conditions, *Int. J. Biomath.*, 7 (2014) (16 pages).
- [12] N. S. Gad, Effects of Hall currents on peristaltic transport with compliant walls, *Appl. Math. Comput.*, 235 (2014) 546 – 554.
- [13] T. Hayat, Z. Nisar, B. Ahmad and H. Yasmin, Simultaneous effects of slip and wall properties on MHD peristaltic motion of nanofluid with Joule heating, *J. Magn. Magn. Mater.*, 395 (2015) 48 – 58.
- [14] A. Ebaid and E. H. Aly, Exact analytical solution of the peristaltic nanofluids flow in an asymmetric channel with flexible walls and slip condition, *Compu. Math. Meth. Med.*, 2013 (2013) (8pages).
- [15] K. Vajravelu, S. Sreenadh and R. Saravana, Combined influence of velocity slip, temperature and concentration jump conditions on MHD peristaltic transport of a Carreau fluid in a non-uniform channel, *Appl. Math. Comput.*, 225 (2013) 656 – 676.
- [16] T. Hayat, M. Rafiq, A. Alsaedi and B. Ahmad, Radiative and Joule heating effects on peristaltic transport of dusty fluid in a channel with wall properties, *Eur. Phys. J. Plus*, 129 (2014) 225.
- [17] S. Nadeem and N. S. Akbar, Influence of radially varying MHD on the peristaltic flow in an annulus with heat and mass transfer, *J. Taiwan Inst. Chem. Eng.*, 41 (2010) 286 – 294.
- [18] R. Ellahi and F. Hussain, Simultaneous effects of MHD and partial slip on peristaltic flow of Jeffrey fluid in a rectangular duct, *J. Magn. Magn. Mater.*, 393 (2015) 284 – 292.

- [19] N. Ali, K. Javed, M. Sajid and O. A. Beg, Numerical simulation of peristaltic flow of a biorheological fluid with shear dependent viscosity in a curved channel, *Comp. Meth. Biomech. Biomed.*, 59(2015) 1 – 14.
- [20] M. Sheikholeslami, M. G. Bandpy, R. Ellahi and A. Zeeshan, Simulation of MHD CuO–water nanofluid flow and convective heat transfer considering Lorentz forces, *J. Magn. Magn. Mater.*, 369(2014) 69 – 80.
- [21] F. M. Abbasi, T. Hayat and A. Alsaedi, Effects of inclined magnetic field and Joule heating in mixed convective peristaltic transport of non-Newtonian fluids, *Bull. Polish. Acad. Sci. Tech. Sci.*, 63 (2015) 501 – 514.
- [22] M. Mustafa, S. Abbasbandy, S. Hina and T. Hayat, Numerical investigation on mixed convection peristaltic flow of fourth grade fluid with Soret and Dufour effects, *J. Taiwan. Inst. Chem. Eng.*, 45(2014) 308 – 316.
- [23] T. Hayat, F. M. Abbasi, M. Al-Yami and S. Monaqueel, Slip and Joule heating effects in mixed convection peristaltic transport of nanofluid with Soret and Dufour effects, *J. Mol. Liq.*, 194 (2014) 93 – 99.
- [24] S. Srinivas and R. Muthuraj, Effects of chemical reaction and space porosity on MHD mixed convective flow in a vertical asymmetric channel with peristalsis, *Math. Comput. Model.*, 54 (2011) 1213 – 1227.
- [25] S. Srinivas, R. Gayathri and M. Kothandapani, Mixed convective heat and mass transfer in an asymmetric channel with peristalsis, *Comm. Nonlinear Sci. Num. Simulation*, 16 (2011) 1845 – 186.